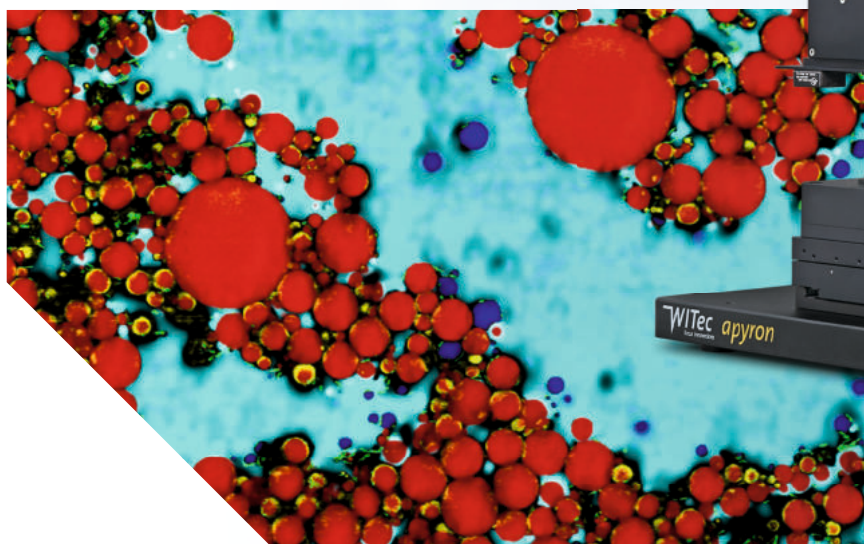


# Virtual Raman Imaging Poster Summit 2020



International Conference for  
Chemical Characterization & Imaging  
September 28<sup>th</sup> – October 2<sup>nd</sup>, 2020



# A Virtual Introduction

Each autumn for the last 16 years, WITec has hosted the Confocal Raman Imaging Symposium. This year, we decided to postpone it due to the ongoing pandemic. It was a very difficult decision for us as the conference is one of the most important events in our calendar, and one that we especially look forward to. It's therefore a great consolation that every speaker we'd invited has confirmed their participation in next year's event, the 17<sup>th</sup> Confocal Raman Imaging Symposium, which will be held in September 2021.

The primary aim of our Symposium is to bring the Raman community together and provide a platform for presenting and discussing the latest developments and applications in Raman imaging microscopy. Scientific exchange is even more important in the current situation, when international travel involves new precautions and complications, but research around the world continues to make rapid progress. With this year's conference postponed, we wanted to offer an alternative forum for the Raman community to engage and interact. Our efforts resulted in the first Virtual Raman Imaging Poster Summit, a one-week online poster session that offered researchers the possibility to share and discuss results from the convenience of their home offices.

We were amazed at how well the format was received. There were about 250 participants and a total of 55 posters covering various fields of application. The enthusiastic response confirmed that scientists are eager to share their recent results and find new modes of engagement with their colleagues. It was also apparent that the online format of the conference gave it a very international character, because it facilitated participation from every global region.

This spring, many researchers had only limited access to their labs, which of course made it challenging to continue performing measurements as usual. We saw that many scientists focused on data analysis in these months and profited from the extensive functionality of our software suite and in particular from our special Home Office License. However, experimental research in laboratories also continues even when the amount of time spent in home office has increased. In line with these developments, WITec launched the new generation alpha300 *apyron* in April. This fully automated confocal Raman microscope can carry out self-alignment and self-calibration to optimize reproducibility and performance. Another advantage is that it can be controlled completely remotely, with only the placement of the sample requiring physical interaction. Thus, even measurements from home offices become possible.

We thank everyone who contributed to the success of the first Virtual Raman Imaging Poster Summit and we hope to welcome many of you next year in Ulm at the 17<sup>th</sup> Confocal Raman Imaging Symposium.

Stay safe and healthy.



Olaf Hollricher and Joachim Koenen  
Managing Directors at WITec GmbH

# Poster Abstracts

## Advanced Materials Analysis

p. 5

## Correlative Imaging Applications

p. 29

## Environmental and Geoscience

p. 35

## Life Sciences, Biomedical and Pharma Research

p. 45

SUBMIT UNTIL  
JANUARY 31

**WITec**  
focus innovations

# WITec Paper Award

The WITec PaperAward recognizes exceptional scientific publications in a peer-reviewed journal that include results and/or images acquired with a WITec microscope system. Scientists from all over the world are encouraged to submit their papers published (print or online) in the current year.

The use of a WITec microscope system should be clearly documented either in the „Materials and Methods“ section of the article or by other supporting documentation.

Each submitted paper is valid for one giveaway and any author of a paper can submit it.

A WITec jury will judge the submitted papers in terms of scientific relevance, data quality and the level of instrument feature utilization. The awards for the three best papers will be given to the first authors.

Once a year, a jury will appoint the winners of the annual award.

Entry deadline is January 31<sup>st</sup> of each year.

## How to contribute:

- 01 Send your paper (PDF format) to [papers@witec.de](mailto:papers@witec.de) and include your full contact information.
- 02 Receive a WITec thank-you gift for each new paper submitted.
- 03 Automatically participate in the WITec Paper Award competition. The first authors of the three best papers will receive a 500 € (GOLD), 300 € (SILVER) or 200 € (BRONZE) Amazon gift card.

Submit new scientific results acquired with a WITec microscope system to be placed in consideration for the WITec Paper Award. Each qualifying paper will automatically compete for the prize and WITec will send a small present to the person that submitted a paper.

## WITec Headquarters

WITec GmbH

Lise-Meitner-Straße 6 . D-89081 Ulm . Germany

Phone +49 (0) 731 140700 . Fax +49 (0) 731 14070200

info@WITec.de . www.WITec.de



# Advanced Materials Analysis

## **Investigation of Properties of ZnO Nanostructures by First- Principals Calculations**

S. OUDJERTLI

Research Center In Industrial Technologies. CRTI. P.O.BOX 64, Cheraga, Algeria, ALGERIA, Algeria

Structural and microstructural properties were investigated by first-principals computing. The ZnO powder as Transparent Ceramics exhibited a hexagonal crystal structure with space group  $P6_3mc$  of ZnO. We applied the present first-principals approach to the electronic structure of the ZnO structures. Band structure and density of states of the phase of crystal ZnO computed using first principal methods, confirmed that pure ZnO is a direct band gap semiconductor when obtained in the B4 type structure phase.

### 3D Stress Mapping and Texture Analysis of Nacre using Correlative Micro-indentation and Piezo-Raman

H.-C. Loh<sup>1</sup>, T. Divoux<sup>1,2,3</sup>, F.-J. Ulm<sup>1,2</sup>, A. Masic<sup>1</sup>

<sup>1</sup>MIT, Department of Civil and Environmental Engineering, Cambridge, MA, United States, <sup>2</sup>CNRS–MIT, MultiScale Material Science for Energy and Environment, Cambridge, MA, United States, <sup>3</sup>Univ Lyon, Ens de Lyon, Univ Claude Bernard, CNRS, Laboratoire de Physique, Lyon, France

Nacre (mother-of-pearl) has been extensively studied for its excellent combination of high stiffness, strength, and toughness. These outstanding mechanical properties have been mostly attributed to the interplay between aragonite platelets ( $\sim 0.5 \mu\text{m}$  thick) and organic matrices in the typical brick-and-mortar structure. Here, we report a new length scale of  $\sim 20 \mu\text{m}$  that contributes to nacre's toughening mechanism, investigated by correlating micro-indentation and piezo-Raman spectroscopy studies. A series of micro-indentation tests with different maximum force is performed on nacre samples, and the images of the indented area (SEM; Figure 1a) are correlated to the crystallographic texture (polarized Raman; Figure 1b) and the stress distribution (piezo-Raman; Figure 1c-d). First, the crystallographic texture analysis shows that stacks of aragonite tablets have the same crystal orientation forming co-oriented aragonite columns with a characteristic dimension of around  $20 \mu\text{m}$ . Then, by correlating piezo-Raman and micro-indentation results, we quantify the residual strain energy associated with the strain hardening capacity of nacre samples. Plotting the residual stress energy stored in the material against the effective indent size, we find that a strain hardening mechanism is activated when the indent size is in the order of the characteristic aragonite column height. Our results show that the co-oriented aragonite columns effectively store energy through cooperative plastic deformation, defining a new length scale of nacre toughening. This work also highlights the effectiveness of correlative SEM-Raman imaging tools in quantifying and mapping the plastic deformation and the 3D residual stress field, as well as analyzing the crystallographic texture with sub-micron spatial resolution.

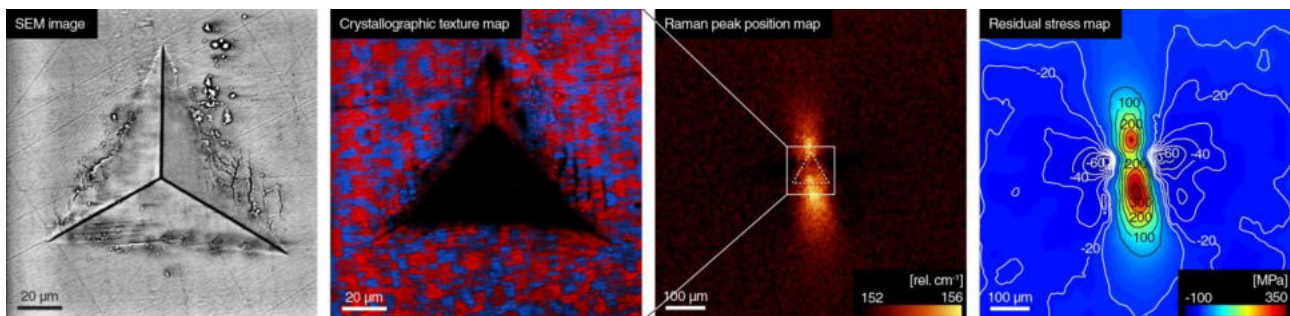


Fig 1 Characterization of an indented nacre sample (a) SEM image (b) Crystallographic texture map; Red and blue colors indicate different crystal orientations (c) Raman peak position map (d) Residual stress map calculated with piezo-Raman calibration

## **Characterization of virgin and ion irradiated graphite surface by Raman spectroscopy**

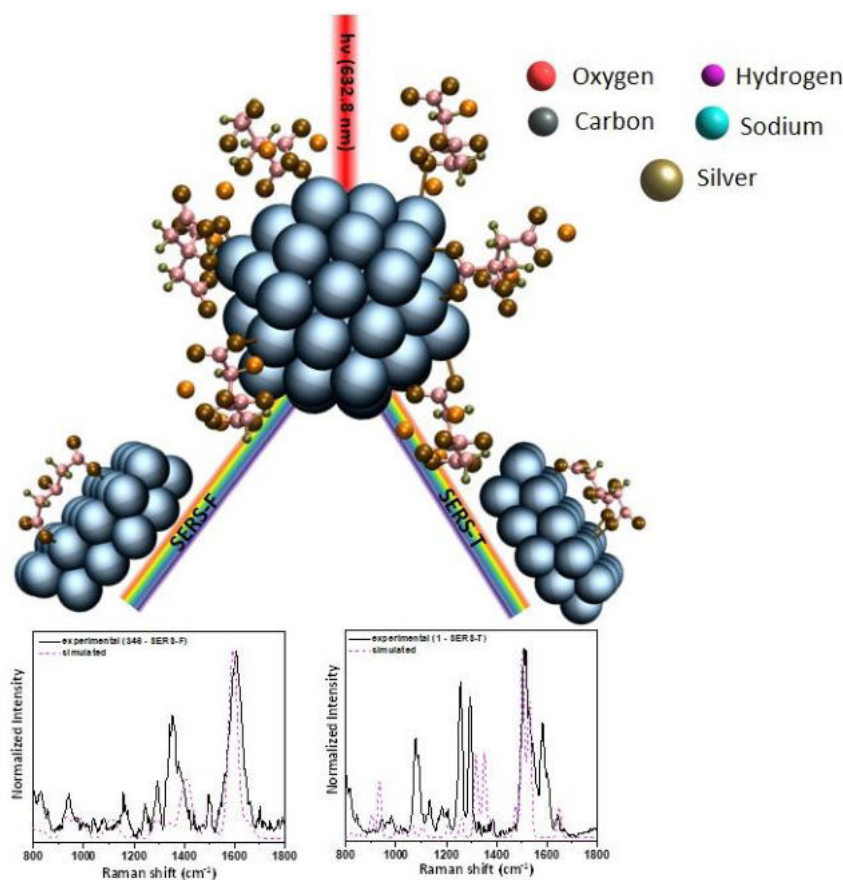
M. Wilczopolska, Ł. Kurpaska, J. Jagielski, M. Frelek-Kozak  
National Centre for Nuclear Research, Otwock, Poland

Graphite due to its good properties such as good thermal conductivity, high melting point and high thermal shock resistant is currently used as a core structural component for High Temperature Gas Cooled Reactor (HTGR). Virgin and ion irradiated graphite was investigated by Raman spectroscopy to characterize materials used in nuclear technologies. Ion irradiation was performed using a 150 keV Ar<sup>+</sup> beam in order to introduce defects in the structure that could be similar to those created by neutrons in the nuclear reactor. First-order Raman spectra were compared. The lattice damage of graphite is evaluated by comparison of the disorder-induced peak ( $\sim 1348 \text{ cm}^{-1}$ ) with respect to the Raman active  $E_{2g2}$  mode peak ( $\sim 1581 \text{ cm}^{-1}$ ). Virgin spectra are significantly different from irradiated graphite surface.

## Towards vibrational tomography of citrate on dynamically changing individual silver nanoparticles

T. Ahuja, K. Chaudhari, G. Paramasivam, G. Ragupathy, J. S. Mohanty, T. Pradeep  
IIT Madras, Chemistry, Chennai, India

This study explored changes in binding modes of the ubiquitous ligand, citrate on silver nanoparticles (AgNPs) using single-particle surface-enhanced Raman scattering (SP-SERS). Single AgNPs of  $50 \pm 10$  nm anchored on clean glass slides, having plasmonic scattering in the regime of 620-670 nm, were monitored for time-dependent SERS with a 632.8 nm excitation laser at  $1.3 \mu\text{W}$  power per nanoparticle. We observed distinct spectra of citrate during time-dependent SERS. A set of 1400 spectra was analyzed by cluster analysis which showed the existence of two major sets of clusters, termed 'SERS-Favorable (SERS-F)' and 'SERS-Transient (SERS-T)' spectra, based on their probability of appearance. These distinct spectra corresponded to a multitude of structures, binding modes, and variants of photocatalyzed products of citrate on the surface of dynamically changing AgNPs. Density functional theory (DFT) simulations were performed to model the structures and binding modes of citrate on an Ag(111) surface and corresponding Raman spectra were computed. Experiments performed with deuterated citrate-capped AgNPs provided additional evidence to understand the shifts in vibrational features obtained in SP-SERS of citrate-capped AgNPs. Our strategy of systematic analysis of time-dependent SP-SERS spectra can probe structural variations, which can be used for reconstruction and vibrational tomography of ligands at the single-particle level.



Towards vibrational tomography of citrate on single AgNP

A paper based on this work is in the process of publication.

## Investigation of inherent stress using confocal Micro Raman in GaN Heterostructure for RF HEMT Applications

R. Kaneriy<sup>1,2</sup>, C. Karmakar<sup>1</sup>, G. Rastogi<sup>1</sup>, R. B. Upadhyay<sup>1</sup>, P. Kumar<sup>1</sup>, A. N. Bhattacharya<sup>1</sup>

<sup>1</sup>Space Application Centre, ISRO, Microelectronics Group, Ahmedabad, India, <sup>2</sup>Indian Institute of Space Science and Technology, Department of Physics, Thiruvananthapuram, India

### Abstract

The influence of AlGa<sub>0.3</sub>N barrier layer and 6H-SiC substrate on inherent stress in GaN heterostructure is investigated using confocal micro Raman measurement. Depth profile measurements were carried out to extract the inherent stress for Al<sub>0.3</sub>Ga<sub>0.7</sub>N/GaN heterostructure on 6H-SiC wafer. It has been reported a valley type inherent stress profile in GaN heterostructure. As we move toward 2DEG from top of AlGa<sub>0.3</sub>N barrier layer, pronounced increase of inherent tensile stress is observed. Furthermore, transition from tensile to compressive stress is found towards the 6H-SiC substrate.

### Method

The inherent stress in growth play a crucial role in the generation of carriers, especially for polarization depended GaN heterostructure. The GaN heterostructure has been grown by MOCVD on c-plane 6H-SiC substrate. Layer stakes, thickness and composition for heterostructure is depicted in inset of Fig. 1(a), which include 60nm AlN nucleation layer, 2 micron GaN buffer layer and 20nm undoped Al<sub>0.3</sub>Ga<sub>0.7</sub>N layer on 6H-SiC. We evaluate heterostructure properties by room temperature micro Raman scattering experiments using WiTec alpha 300 Raman confocal microscope equipped with the 532 nm laser as the excitation light source, 1200 lines/mm grating, and 100 X objective lens. The Raman spectra give the information about lattice vibration and corresponding stress in the material. We adopted Fig. 1(a) measurement methodology to extract the true nature of inherent stress in depth profiling.

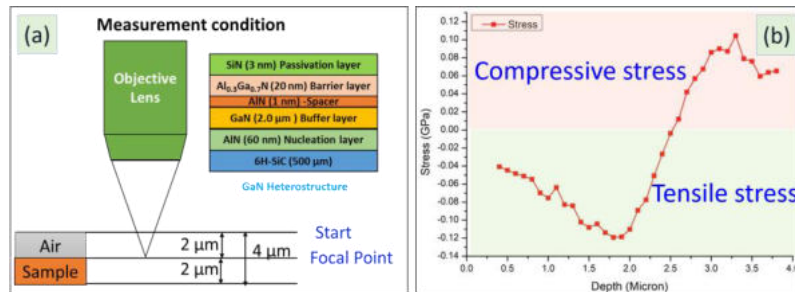


Fig.1 (a) Measurement method (Inset: Investigated GaN Heterostructure), (b) Depth profile of Inherent stress in GaN Heterostructure

### Results

Room temperature Raman spectra of the GaN heterostructure are measured and variation in E<sub>2</sub> (high) phonon peak throughout 4 micron depth extracted. The E<sub>2</sub> peak in GaN is very much sensitive to stress in the films.

The relation between biaxial stress  $\sigma_{xx}$  and Raman shift  $\Delta\omega$  (568 cm<sup>-1</sup> select GaN strain free E<sub>2</sub>-High phonon peak [2]) is given by[1,2]

$$\Delta\omega = K\sigma_{xx} \quad (1)$$

where K is linear stress coefficient.

For GaN on 6H-SiC,  
K=2.7 cm<sup>-1</sup>/GPa [1,2]

The inherent stress calculated using equation (1) is depicted in Fig.1(b).

### Conclusion:

The influence of AlGa<sub>0.3</sub>N barrier layer and 6H-SiC substrate on inherent stress in GaN heterostructure has been calculated through E<sub>2</sub>-high phonon peak shifting. This study can be used to improve GaN HEMT devices performance for RF applications.

### References

- [1] J.-M. Wagner, et al. Applied Physics Letters 77, 346 (2000)  
[2] V. Yu. Davydov, et al. Appl. Phys. 82, 5097 (1997)

### Acknowledgment

We are thankful to Hitesh Mamgain, Application Scientist, WITec, GmbH for providing Raman facility

## Cascaded nanooptics to probe microsecond atomic-scale phenomena

M. Kamp

University of Cambridge, Physics, Cambridge, United Kingdom

Plasmonic nanostructures can focus light far below the diffraction limit, and the nearly thousandfold field enhancements obtained routinely enable few- and single-molecule detection. However, for processes happening on the molecular scale to be tracked with any relevant time resolution, the emission strengths need to be well beyond what current plasmonic devices provide. Here [1], we develop hybrid nanostructures incorporating both refractive and plasmonic optics, by creating SiO<sub>2</sub> nanospheres fused to plasmonic nanojunctions. Drastic improvements in Raman efficiencies are consistently achieved, with (single-wavelength) emissions reaching  $10^7$  counts·mW<sup>-1</sup>·s<sup>-1</sup> and  $5 \times 10^5$  counts·mW<sup>-1</sup>·s<sup>-1</sup>·molecule<sup>-1</sup>, for enhancement factors  $>10^{11}$ . We demonstrate that such high efficiencies indeed enable tracking of single gold atoms and molecules with 17-μs time resolution, more than a thousandfold improvement over conventional high-performance plasmonic devices. Moreover, the obtained (integrated) megahertz count rates rival (even exceed) those of luminescent sources such as single-dye molecules and quantum dots, without bleaching or blinking.

[1] M. Kamp *et al.* PNAS 117, p. 14819-14826 (2020).

## **On using statistical Raman Spectroscopy for lithium battery materials characterization**

D. Pelegov<sup>1</sup>, B. Slautin<sup>1</sup>, A. Koshkina<sup>2</sup>

<sup>1</sup>Ural federal university, Institute of Natural Sciences and Mathematics, Ekaterinburg, Russian Federation, <sup>2</sup>Institute of Solid State Chemistry UB RAS, Ekaterinburg, Russian Federation

Lithium battery (LB) is a cornerstone element of the today's global economy. About two decades ago, LB enabled the genesis of portable electronics industry. Today, it plays the crucial role in the global transition toward electromobility and renewable energy generation. And the Nobel prize in Chemistry 2019 awarded jointly to John B. Goodenough, M. Stanley Whittingham, and Akira Yoshino "for the development of lithium-ion batteries" features its importance both for science and industry.

Raman Spectroscopy is a rather common tool for structural characterization of LB electrode materials [1], but it is usually considered as an auxiliary one. Generally speaking, there are three most popular applications of Raman Spectroscopy for LB electrode materials: 1) target phase validation, 2) structural characterization of carbon additive, and 3) in-situ studies during lithium intercalation and deintercalation. We believe that there is some room to grow and Raman spectroscopy usage for electrode material characterization can be more intensive.

In this presentation, the alternative big-data or statistical approach is discussed and its application for defects and local heterogeneities probing is proposed. For the first time, the idea of using the statistical analysis of multiple Raman spectra for quality control of LB electrodes was proposed in 2001 in paper [2]. Unfortunately, this idea was not adopted by LB community, but later the similar approach was used for carbonaceous materials studies [3,4]. Recently, we have revived this approach and demonstrated its advantages for heterogeneity characterization of LB electrodes. In order to discuss all the peculiarities of Raman Spectroscopy studies in electrode materials, we will focus on two case studies. First, this statistical approach will be used for the advanced structural defect characterisation in pristine lithium titanate ( $\text{Li}_4\text{Ti}_5\text{O}_{12}$ ) with spinel structure [5]. Second, Raman spectroscopy will be used for structural and morphological characterization of carbon coverage efficiency in LTO-C composites [6].

### References

- [1] Baddour-Hadjean R., Pereira-Ramos J.-P. *Chem. Rev.* (2010) **110**, 1278
- [2] Panitz J. C., Novák P., *J. Power Sources* (2001) **97–98**, 174.
- [3] Beyssac O. et al., *Spectrochim. Acta Part A Mol. Biomol. Spectrosc.* (2003) **59**, 2267.
- [4] Englert J. M. et al., *ACS Nano* (2013) **7**, 5472.
- [5] Pelegov D.V. et al., *J. Power Sources* (2017) **346**, 143.
- [6] Pelegov D.V. et al., *J. Raman Spectrosc.* (2019) **50**, 1015.

## Chemical Vapor Deposition and Characterization of Transition Metal Chalcogenide Heterostructures

L. Peters<sup>1,2</sup>, C. Ó Coileáin<sup>1,2</sup>, C. Cullen<sup>1,2</sup>, R. Siris<sup>3</sup>, G. S. Duesberg<sup>1,2,3</sup>, N. McEvoy<sup>1,2</sup>

<sup>1</sup>Trinity College Dublin, School of Chemistry, Dublin, Ireland, <sup>2</sup>CRANN, Dublin, Ireland, <sup>3</sup>Universität der Bundeswehr München, Institute of Physics, München, Germany

2D materials are promising materials for numerous electronic applications. Especially transition metal dichalcogenides are of interest as these have a range of properties varying from metallic to semi-conducting depending on layer number. This suggests the amazing prospect of creating electronic devices solely from 2D materials through the use of heterostructures. Heterostructures of two dissimilar TMDs result into devices with atomically sharp and clean interfaces in which the properties of the material can be tuned and the band gap can be aligned<sup>1,2</sup>.

In this work a single-step chemical vapor deposition (CVD) growth method is developed in which a micro-reactor is used to synthesize MoSe<sub>2</sub>/WSe<sub>2</sub> and MoS<sub>2</sub>/WS<sub>2</sub> heterostructures<sup>3</sup>. This growth method allows the formation of both lateral and vertical heterostructures offering a large range of possible device architectures. In case of MoSe<sub>2</sub>/WSe<sub>2</sub> automatically-thin pn-junctions can be created without further processing steps due to the combination of n-type MoSe<sub>2</sub> and ambipolar WSe<sub>2</sub>.

The quality and properties of the synthesized materials were intensely studied by various characterization techniques such as (low-frequency) Raman spectroscopy, photoluminescence, spectroscopy, x-ray photoelectron spectroscopy and atomic force microscopy (AFM). Advanced AFM modes such as conductive AFM and Kelvin probe force microscopy offered deeper insight into the properties of these materials.

1 A. K. Geim and I. V Grigorieva, *Nature*, 2013, **499**, 419–25.

2 A. V. Kretinin, Y. Cao, J. S. Tu, G. L. Yu, R. Jalil, K. S. Novoselov, S. J. Haigh, A. Gholinia, A. Mishchenko, M. Lozada, T. Georgiou, C. R. Woods, F. Withers, P. Blake, G. Eda, A. Wirsig, C. Hucho, K. Watanabe, T. Taniguchi, A. K. Geim and R. V. Gorbachev, *Nano Lett.*, 2014, **14**, 3270–3276.

3 M. O'Brien, N. McEvoy, T. Hallam, H.-Y. Kim, N. C. Berner, D. Hanlon, K. Lee, J. N. Coleman and G. S. Duesberg, *Sci. Rep.*, 2014, **4**, 7374.

## Laser-induced LiFePO<sub>4</sub> decomposition

A. Ryabin, D. Pelegov

Ural Federal University, Institute of natural sciences and mathematics, Ekaterinburg, Russian Federation

During the last decade, the lithium battery industry is thriving due to steady demand from automobile and energy industries. This maturing phase strongly needs production scale growth and cell price decreasing. Both trends increase the role of quality control (QC) tools, especially ones, suitable for industrial applications. Raman spectroscopy (RS) is one of the most promising candidates for industrial QC tools due to relatively low acquisition times, inexpensive equipment and ability to be built-in production lines. So, we are promoting the idea of using Raman spectroscopy for popular electrode material lithium iron phosphate (LiFePO<sub>4</sub> or LFP). But there is a significant problem of LFP characterization by Raman spectroscopy – the laser-induced decomposition.

To understand processes resulting in LFP decay under the action of laser irradiation, we used the combination of statistical and local approaches to Raman spectroscopy. First, we carried out 26 measurements on powder samples with different values of laser power. Each measurement represents itself as a scan (mapping) of the 10<sup>7</sup> 10 μm region and consisted of 100 individual Raman spectra. It was expected that the probability of LFP decay will rise with increasing laser power. However, the results present an irregular dependence. The observed peculiarity of LFP decay is discussed in the terms of several stages of the decomposition kinetics [1]. Second, the decomposition of single particles was studied. We measured Raman spectra using 1.59 mW power for 75 single particles sedimented on Si substrate. Such an approach allowed to reveal different scenarios of laser-induced phase transitions and estimate the stability of major band parameters to the continuous action of laser irradiation.

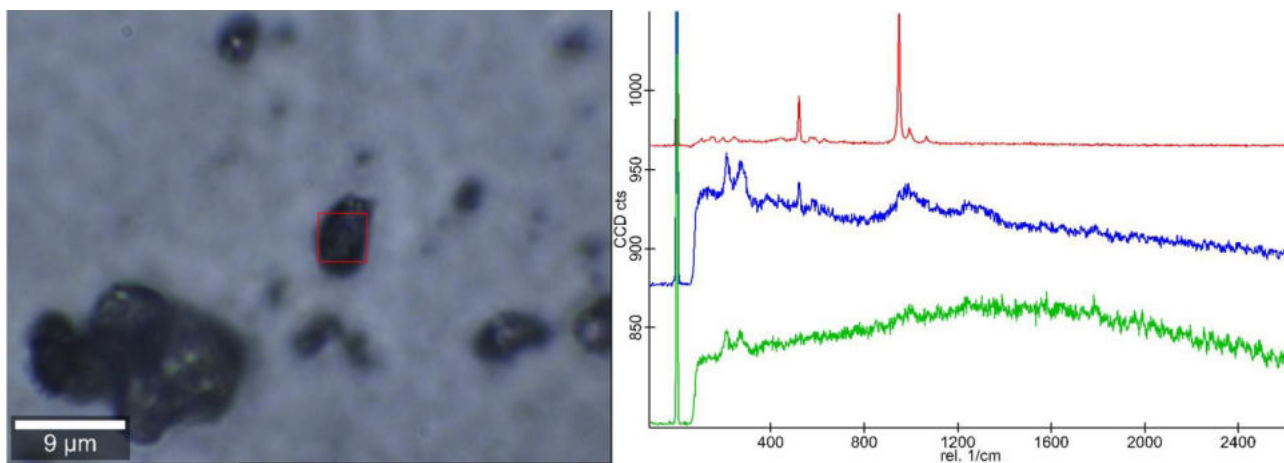


Photo of decomposed single particle and typical spectra of Raman image scan for it

### References:

[1] A. A. Ryabin, B. N. Slautin, D. V. Pelegov, Three-stage kinetics of laser-induced LiFePO<sub>4</sub> decomposition, *J. Raman Spectrosc.* (2019). doi: 10.1002/jrs.5803

## Non-contact evaluation of carrier concentration for power electronics

A. Myalitsin, O. Milikofu  
Nissan ARC, Yokosuka, Japan

With rapid growth of wide-band-gap semiconductors for efficient use of energy everywhere from home electronics to high speed railways and heavy machinery for mining and construction, the need for a fast and non-destructive method to evaluate the raw materials, as well as device quality, also increases. While currently SIMS (secondary ion mass spectroscopy) is the most sensitive method to evaluate the dopant concentration in semiconductor surfaces, it is destructive and therefore unfavorable to use between device manufacturing steps. On the contrary, Raman spectroscopy is a fast, contact-free and non-destructive method.

We used the confocal microscope “Alpha 300R” in back-scattering geometry to map the Raman signal of an n-type doped 4H-SiC epitaxial layer on a 4H-SiC wafer as a function of depth (figure 1a). It is well-known that the  $A_1$  longitudinal optical (LO) phonon around  $980\text{ cm}^{-1}$  shows a significant peak shift and asymmetric broadening as a function of dopant concentration, due to phonon-plasmon coupling. [1] As the concentration of free electrons increases, the plasmon frequency shifts to higher wavenumbers and the LO plasmon-coupled mode (LOPC) becomes asymmetrically broadened, while shifting to higher wavenumbers. This broadening has been observed and modelled for single crystal 4H-SiC. [2-4] However, in the case of epitaxially grown films, the sample cannot be considered uniform. Indeed, with increasing depth we see an increase in free electron concentration at the interface (figure 1b). Therefore, special care should be taken when applying the LOPC model to epitaxial wafers. Here we show a method for routine estimation of free carrier concentration based on confocal Raman imaging of a sample surface/depth, and fitting of the experimental Raman LO phonon line shape to theory.

[1] G. Irmer, V. V. Toporov, B. H. Bairamov and J. Monecke, *Physica Status Solidi (b)*, 1983, **119**, 595–603.

[2] S. Nakashima, T. Kitamura, T. Kato, K. Kojima, R. Kosugi, H. Okumura, H. Tsuchida and M. Ito, *Applied Physics Letters*, 2008, **93**, 121913.

[3] H. Harima, S. Nakashima and T. Uemura, *Journal of Applied Physics*, 1995, **78**, 1996–2005.

[4] J. C. Burton, L. Sun, M. Pophristic, S. J. Lukacs, F. H. Long, Z. C. Feng and I. T. Ferguson, *Journal of Applied Physics*, 1998, **84**, 6268–6273.

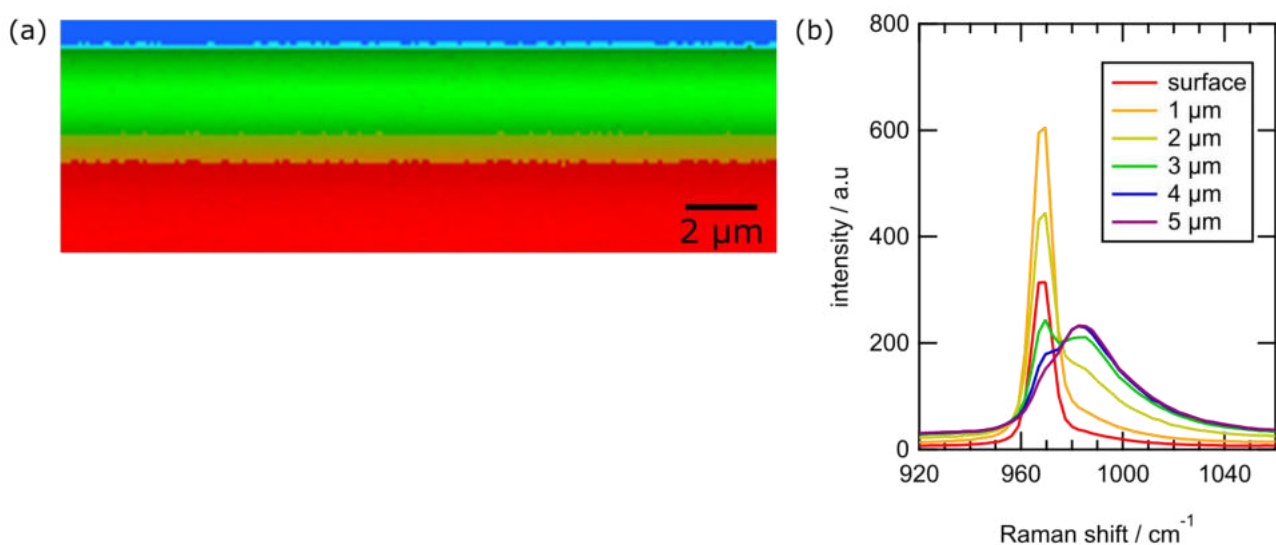


Figure 1: (a) Depth profile of the n-doped 4H-SiC wafer (red), with the undoped epitaxial layer on top (green). (b) Spectra of the LOPC mode as a function of depth.

## Raman and Photoluminescence study in order to determined the aluminum concentration of $\text{Al}_x\text{Ga}_{1-x}\text{N}$

L. MARTINEZ-ARA<sup>1</sup>, P. MALDONADO-ALTAMIRANO<sup>2</sup>, J. AGUILAR-HERNANDEZ<sup>1</sup>, M. HERNANDEZ-PEREZ<sup>3</sup>, G. CONTRERAS-PUENTE<sup>1</sup>

<sup>1</sup>NATIONAL POLYTECHNIC INSTITUTE, PHYSICS, MEXICO, Mexico, <sup>2</sup>CINVESTAV-NATIONAL POLYTECHNIC INSTITUTE, MEXICO, Mexico, <sup>3</sup>NATIONAL POLYTECHNIC INSTITUTE, CHEMESTRY, MEXICO, Mexico

$\text{Al}_x\text{Ga}_{1-x}\text{N}$  films on different substrates, Si (111),  $\text{Al}_2\text{O}_3$  (0001) and amorphous quartz were grown by Pulsed Laser Deposition (PLD). A Nd-YAG laser tuned at 1064 nm wavelength, 12 ns pulse duration and a repetition rate of 50 Hz, was used for the ablation process. The energy of the laser beam focused at the target surface was 50 mJ/pulse. Aluminum concentration was determined by photoluminescence (PL) and Raman spectroscopy. Photoluminescence (PL) measurements were carried out with a He-Cd laser as exciting light, tuned at 325 nm, with a power of 40 mW. The PL at 10 K shows that the yellow band (YL) has a shift of 170 meV at higher energy in the ternary in comparison with the gallium nitride (GaN). Such shift of the PL maximum together with the widening of the YL band is related to the formation of the ternary compound. Raman spectra were measured at room temperature by using a He-Ne laser, 633 nm, it with an output power of 30 mW, in a LabRam HR Evolution system. The Raman spectra show peaks at 569 and 655  $\text{cm}^{-1}$  modes associated to GaN and AlN respectively, and a peak at 772  $\text{cm}^{-1}$ , this frequency corresponds to the vibrational mode  $A_1(\text{LO})$ , this increases continuously from the mode of GaN to the corresponding  $A_1(\text{LO})$  mode of the AlN when the aluminum concentration increases. Beginning with displacement of the vibrational mode the aluminum concentration was determined, it turned out to be 15 %.

## **Confocal Raman imaging of ferroelectric domain structure in KTA single crystals in the bulk**

A. Akhmatkhanov, M. Chuvakova, E. Greshnyakov, V. Shur

Ural Federal University, School of Natural Sciences and Mathematics, Ekaterinburg, Russian Federation

The single crystals of potassium titanyl phosphate (KTiOPO<sub>4</sub>, KTP) family [1] have long been recognized as one of the main materials of nonlinear optics. These uniaxial ferroelectrics are commonly used for creation of the tailored domain structures (domain engineering). It implies that the efficiency of nonlinear optical interactions in these crystals can be improved further by periodical poling for realization of quasi-phase matching conditions. The potassium titanyl arsenate (KTiOAsO<sub>4</sub>, KTA) possesses the properties outperforming KTP which resulted in creation of periodically poled KTA crystals (PPKTA) for various nonlinear optical applications [2]. The periodical poling in KTA consists in application of electric field pulse to the photolithographically defined stripe electrodes to form the precise periodical domain pattern [1]. The undesirable pronounced domain broadening out of the electrodes in KTA crystals requires the deep knowledge of domain kinetics during poling process which implies the possibility of domain structure imaging in the bulk.

The confocal Raman microscopy (CRM) has shown to be a powerful technique for imaging of domain structure in the bulk [3] based on the detection of the shifts of certain Raman peaks on the domain walls. It has been used previously for domain structure imaging in other ferroelectrics but never applied to the KTA crystals. The model quasi-regular streamer structure formed in KTA after partial polarization reversal (field 2.6 kV/mm, pulse duration 10 ms) has been visualized by CRM using Alpha AR300 (WITec, Germany). The incident laser beam was linearly polarized along [010] crystallographic direction. The Raman spectrum in KTA at the domain wall and in the bulk differed by the intensity and the position of the peaks near 675 cm<sup>-1</sup> and 730 cm<sup>-1</sup>. We have used the shift of the peak 730 cm<sup>-1</sup> for domain wall imaging as the most sensitive. The domain structure imaging with spatial resolution down to 350 nm has been demonstrated.

The equipment of the Ural Center for Shared Use "Modern Nanotechnology" Ural Federal University was used. The research was made possible by support from President of Russian Federation Grant for young scientists (grant No. MK-1217.2019.2) and by Russian Foundation for Basic Research (grant No. 18-29-20077-mk).

[1] V. Ya. Shur et al, *Ferroelectrics* 496, 49(2016)

[2] A. Zukauskas et al, *Opt. Mater. Express* 3, 1444(2013)

[3] V. Ya. Shur et al, *J.Appl.Phys.* 116, 066802(2014)

## **Dentin-Dental Adhesive Interface Characterization by Raman Microscopy and Atomic Force Microscopy**

B. Anich<sup>1</sup>, B. Dippel<sup>2</sup>, H. Loll<sup>1</sup>, A. Lopez<sup>1</sup>, G. Mishra<sup>2</sup>, M. Moos<sup>2</sup>, C. Thalacker<sup>1</sup>

<sup>1</sup>3M Deutschland GmbH, 3M Oral Care, Seefeld, Germany, <sup>2</sup>3M Deutschland GmbH, Corporate Research Analytical Laboratory, Neuss, Germany

Dental adhesives are used for dental restorations. In dental restoration, a dentin-adhesive interface typically forms a strong bond between the dentin and composite material. The quality of a dental restoration depends strongly on the properties of a hybrid layer which is formed between the dentin and the adhesive. This hybrid layer consists of a demineralized dentin zone which is infiltrated with adhesive. Demineralization can be accomplished by an additional etching step (total-etch, TE) of the dentin or by self-etch (SE) adhesives.

In this study, we investigated the morphology and chemical nature of the dentin-adhesive interface of an experimental and a commercial Scotchbond Universal (3M) adhesive.

### **Methods:**

The labial surface of bovine incisors was ground to expose dentin and treated with the experimental or the commercial Scotchbond Universal (3M) adhesive in total etch (TE) or self-etch (SE) modes according to manufacturers' instructions.

A 1 mm thick layer of a composite material (Filtek™ Z250 (3M) A3) was placed on the adhesive and cured (Elipar™ S10, 3M). Samples were ground perpendicular to the bonded surface.

The interfaces were investigated with confocal Raman microscopy (Witec 300R with a 100X objective, NA 0.9; excitation wavelength: 532nm) and Atomic Force Microscopy (AFM) (Dimension Icon, Bruker)

### **Results:**

AFM images and Raman linescans were recorded from dentin-adhesive-composite interfaces. Raman linescans of the interface composite-adhesive layer-hybrid layer-dentin were recorded with high lateral resolution. For each sample, a distinct adhesive and a hybrid layer were detected. Raman microscopy revealed full adhesive penetration of the hybrid layer.

### **Conclusions:**

- \* Micro-Raman and AFM results complement each other.
- \* Raman Microscopy and AFM show that the experimental adhesive has a similar interaction with dentin as clinically proven Scotchbond Universal™ (3M) adhesive
- \* Both adhesives achieved complete infiltration of the hybrid layer
- \* The hybrid layer was significantly thicker for total-etch vs self-etch samples.
- \* There was no significant difference for hybrid layers between experimental and commercial adhesive when used in the same etching mode.
- \* The experimental adhesive afforded similar adhesive layer thickness as the commercial Scotchbond Universal™ (3M) adhesive in TE mode, and lower adhesive layer thickness in SE mode

## **Imaging the distribution of additives in different materials using Raman microscopy**

J. Swart, C. van Hoorn

Nouryon, ECG-MAS, Deventer, Netherlands

At ECCD (Expert Capability Centre Deventer), part of Nouryon, a chemicals manufacturer, Raman imaging is used to provide insight in the distribution of organic and inorganic additives in all kinds of materials, e.g. polymers, paints, coatings and chemicals. The distribution of components in the matrix plays a crucial role in the functioning and end properties of a material.

Our poster will explore two different applications of using Raman microscopy to study the distribution of additives in a material.

In the first example, we show how this technique can be used to study the migration properties of small wax particles in a coating. These wax particles function as a supply source for migration of wax to the surface, herewith enhancing protection against fouling and mechanical damage.

The second example shows Raman imaging used as a tool to visualize the homogeneity of peroxide-phlegmatizer particles. Phlegmatizers are chemical components used to reduce the hazards of highly reactive peroxides during transport and while in storage. Preferably, the two components are mixed homogeneously. Raman imaging offers a fast method to investigate the distribution of peroxide and phlegmatizer, on both the surface and the inside of the particles.

In both examples the 'cluster analysis' data evaluation tool was used to identify the different components present in the investigated materials. In the second example, a statistical method was applied to enable comparison of different mixing technologies in a semi quantitative way.

## Structural Study of PA66/PA612 Blends for Automobile Applications

O. Milikofu, A. Myalitsin, A. Tominaga, A. Kato  
Nissan ARC, Ltd., Nanomaterial Analysis Group / Nanospectroscopy, Yokosuka, Japan

Common polyamides like PA6 and PA66 are attractive materials for automobile industry due to ease-to-process, light weight and added mechanical strength in thermoplastic composites, lacking, however, sufficient hydrolytic and chemical stability. In comparison to PA66, PA612 absorbs only 1/2 ~ 1/3 amount of water [1,2], but lacks strength and is much more expensive. Blends of PA612 with PA66 were reported to have improved mechanical properties and stability [3,4]. Based on thermal studies, phase separation was suggested, however, was never confirmed directly.

In this study, we used PA66:PA612 blends with weight ratio 10:0, 7:3, 3:7 and 0:10, kindly supplied by AsahiKasei Corporation. Confocal Raman microscope alpha 300R (WITec GmbH, 532nm) in back-scattering geometry was used to obtain 2D and 3D maps of the samples. Data were processed and analyzed with Project FIVE software.

First, Raman spectra of pure PA66 and PA612 samples showed small differences in the 900-1700  $\text{cm}^{-1}$  range (amide,  $\text{CH}_2$  and CCO groups). Instead, the shift of the spectral weight (center-of-mass) of  $\text{CH}_2$  stretching region (2850-2950 $\text{cm}^{-1}$ ) was more prominent. This parameter was used in the blends to confirm validity of the basis analysis with component de-mixing. Two basis components were identical to pure PA66 and PA612 spectra, and their calculated relative concentration was consistent with weight ratio. Clear sea-island structure was observed.

Second, we compared crystallinity of the samples. The 7:3 blend had denser and more regular hydrogen bond network than the 3:7 one. It appears that the minor component worked as a seed for crystallization of the major component. Within the blends, PA66 domains had consistently higher crystallinity than PA612 ones.

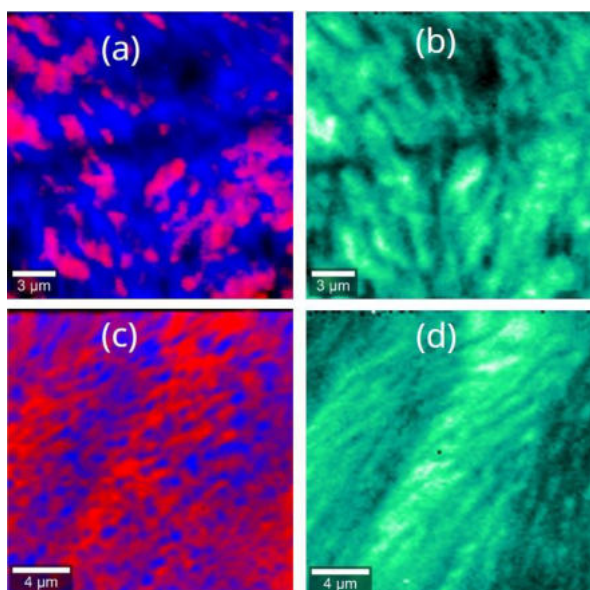
Finally, the solubility parameter  $d$ , calculated from the cohesive energy and mole volume of the repeating units, was found to be 27.975 and 24.887 ( $\text{J}/\text{cm}^3$ )<sup>1/2</sup> for PA66 and PA612, respectively. The values are close but not the same, and taking into account hydrogen bonding, phase separation can be explained.

1 ARKEMA Corporation, Polyamide data sheet, 2015 (in Japanese).

2 S. Goto, H. Yamazaki, M. Nozaki, *DENSO Technical review*, 2009, **14**, 89 (in Japanese).

3 D. Rusu, M. Rusu, Polyamide-based blends, in *Handbook of Polymer Blends and Composites*, 2003, **4a**, 201.

4 T.S. Ellis, *Polymer*, 1992, **33**, 1469.



Structure (red: PA66, blue: PA612) and hydrogen bond network in 3:7 (a, b) and 7:3 (c, d) blends

## **Individual flakes and films of graphene oxide patterned by laser using Raman spectroscopy and atomic force microscopy**

L. PEREZ<sup>1</sup>, F. FIORAVANTI<sup>1</sup>, N. BAJALES LUNA<sup>2</sup>, G. LACCONI<sup>1</sup>

<sup>1</sup>INFIQC-CONICET, Universidad Nacional de Córdoba, Dpto. Fisicoquímica, Facultad de Ciencias Químicas, Córdoba, Argentina, <sup>2</sup>IFEG-CONICET, Universidad Nacional de Córdoba, Facultad de Matemática, Astronomía, Física y Computación, Córdoba, Argentina

Raman spectroscopy was used for quality control and identification of graphene oxide (GO) flakes, but it is able to generate a laser-induced reduction process during the spectroscopic characterization. However, only few recent reports have advised about potential changes induced by laser irradiation, even at low power, during the measurements of such systems. Thus, an overview of this phenomenon is urgently required because it leads to new alternatives for obtaining hybrid surfaces of thin two-dimensional materials, which are useful for diverse applications. Individual flakes and films of GO were deposited on silicon oxide and exposed to visible laser radiation during characterization by micro-Raman spectroscopy. Noticeable topography modifications on both GO individual sheet and film surfaces were observed in the optical image, recorded after spectroscopic measurements. These surface morphology modifications together with an apparent thickness change were induced by the visible radiation in the graphene-based coating. Likewise, chemical changes of the oxygen functional groups ( $sp^3$  carbon defects in the GO structure) were recognized, identifying the decrease of the oxygen content by means of X-ray photoelectron spectroscopy, which evidenced the formation of reduced graphene oxide (rGO) in the trace generated by the laser, when a sample movement control is available. Differences of characteristics between components GO and rGO in the hybrid were supported also by SEM, dark field microscopy and NSOM images. Comparison between laser-induced effects in supported GO films and GO flakes, as well as a correlation with changes observed in Raman spectra and temporal evolution were performed. This study contributes to the quality control of supported GO flakes and films because it provides information about physical damage produced by the laser radiation during Raman measurements. In addition, the combined AFM-Raman spectroscopy research strategy here employed, introduces a simple lithographic method to obtain GO-rGO hybrid materials by using a continuous visible laser to pattern GO flakes and films.

Keywords: Lithographic pattern; graphene oxide; microchannels; Raman imaging; atomic force microscopy.

## Characterization of thiolate-protected QDs on acrylic and silicone-based elastomers films

P. Jofré-Ulloa<sup>1,2</sup>, M. Alegía<sup>1,3</sup>, D. Guzmán de la Cerda<sup>2,4</sup>, C. González-Henríquez<sup>1,2</sup>

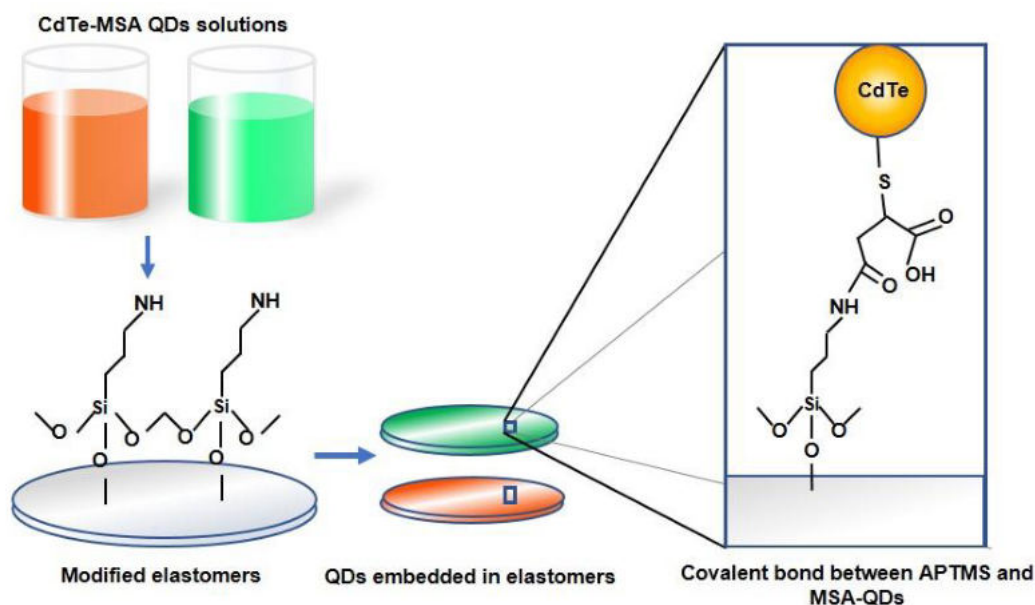
<sup>1</sup>Universidad Tecnológica Metropolitana, Departamento de Química, Santiago, Chile, <sup>2</sup>Universidad Tecnológica Metropolitana, Programa Institucional de Fomento a la Investigación, Desarrollo e Innovación (PIDi), Santiago, Chile, <sup>3</sup>Universidad Tecnológica Metropolitana, Doctorado en Ciencias de Materiales e Ingeniería de Procesos, Santiago, Chile, <sup>4</sup>Universidad Mayor, Centro de Nanotecnología Aplicada, Santiago, Chile

The creation and development of new materials with highly adjustable properties is a rapidly expanding field due to the significant technological advances in recent decades. Some smart materials, such as dielectric elastomers (DE), can change their electromechanical characteristics by applying electric fields, which makes them ideal for transducers.

The incorporation of Quantum Dots (QDs), semiconductor nanocrystals with optoelectronic properties depending on their size, shape, and chemical composition could modify their optoelectromechanical properties. These properties provide a wide range of applications, especially in optoelectronic devices and biomedicine, where the use of cadmium chalcogenides QDs have been intensively investigated. Modifying polymers with nanoparticles (NPs) to form polymer nanocomposites (PNCs) capable of responding to specific stimuli has been a major field of research.

In this work, we used PDMS and 3M VHB 4910 (AR) as substrates to obtain new PNC materials. Both DEs materials have been modified by different methods with CdTe-MSA QDs obtained from organometallic synthesis, but not by aqueous synthesis. The surface was modified following UV-ozone exposure and subsequent formation of a Self-Assembled Monolayer (SAM) with (3-aminopropyl)trimethoxysilane (APTMS), which served to anchor the thiol capped-QDs to the elastomer.

The covalent bond between the thiol coating and the SAM was verified by confocal Raman spectroscopy. Considering the QDs fluorescence, samples for Raman spectra were characterized on gold surfaces, for quenching, and a lower energy laser ( $\lambda = 784 \text{ nm}$ ) resulting in the corresponding spectra of the modified PNCs. The covalent bond was confirmed on samples APTMS-QDs of different sizes, corresponding to amide signals.



Scheme incorporation of quantum dots in elastomer films and the representation of the covalent bond forming an amide between the organic coating and the SAM.

## **Nanofabrication of Metal Free SERS Substrate**

A. Kundu, R. Rani, K. Hazra  
Institute of Nano Science and Technology, Mohali, India

Black Phosphorous (BP), having intrinsic in-plane ferroelectric properties may have inherent capability of SERS response and could be considered a replacement of metal nanoparticles based SERS substrate. A simple one-step process has been demonstrated for controlled nano-structuring and rapid prototyping on BP flake to develop metal free SERS substrate by low power focused laser irradiation. The effect of focused laser irradiation on the surface morphology of pristine BP flakes has been thoroughly investigated by real time Raman spectroscopic measurements and corresponding AFM height profiling, which confirms that the proposed laser irradiation technique has more advantages over conventional lithography process and free from undesired contamination. For 532 nm laser line, the minimum laser power needed to create a nano-void on BP flake is 25 mW (Power density  $\sim 15.62 \times 10^5 \text{ W/cm}^2$ ) with 5 sec exposure time where the etching rate is controllable by the laser power and exposure time. By analyzing the geometrical shape of the nano-void, created due to laser irradiation, it is possible to identify the armchair and zigzag direction of BP flake. Experimental results reveal that by controlling the exposure time and laser power it is possible to perform layer by layer thinning of BP flakes. The proposed thinning process of the BP flake does not alter the pristine quality and no signature of oxidation is found in the Raman spectra, which signifies the reliability of this low power laser irradiation technique towards the future of nano-fabrication of BP based devices. Controlled formation of nano-voids array on few layer BP flake induces enhanced local electric field (hot spots) at the vicinity of the nano-voids, resulting in  $\sim 30\%$  Raman intensity enhancement. Such nano-voids induced hotspots on BP flake open up a new species of metal free SERS substrate, demonstrating pronounced enhancement in Raman signal of Rhodamine B as high as of the order of  $\sim 10^6$  and with a limit of detection (LOD) upto  $\sim 10 \text{ nM}$ .

## Synthesis of silver nanoparticles using Silybin B or silibinin as reducing agents induced by light and the raman characterization study

A. Solís-Gómez<sup>1</sup>, R. A. Guirado-Lopez<sup>2</sup>, J. G. Bañuelos-Muñetón<sup>1</sup>, J. M. Saniger<sup>1</sup>, M. E. Mata-Zamora<sup>1</sup>

<sup>1</sup>Universidad Nacional Autónoma de México, Instituto de Ciencias Aplicadas y Tecnología, Mexico city, Mexico,

<sup>2</sup>Universidad Autónoma de San Luis Potosí, Instituto de Física, San Luis potosi, Mexico

Silybin is an antihepatotoxic polyphenolic substance isolated from the milk thistle plant, used for the treatment of cirrhosis, hepatitis, and alcohol-induced liver disease which is also under study because of its possible neuroprotective effect in Parkinson's disease. Silibinin is a mixture of silybin A and silybin B in a 1:1 ratio. The reduction of silver nitrate with silybin B or silibinin ( $10^{-5}$ ,  $10^{-6}$ , M) without additional steps produced silver nanoparticles can be used as SERS substrates. The SERS enhancement of these silver nanoparticles was tested using the same reductors.

The structure and composition of the silver nanoparticles were characterized by UV-visible spectroscopy, atomic force microscopy (AFM) and Raman spectroscopy, using a 532 nm laser. The evolvment of a characteristic surface plasmon extinction spectrum in the range of 420 nm to 480 nm indicates the formation of silver nanoparticles after mixing silver nitrate solution and silybin B or silibinin. Raman maps were acquired and analysed to identify silybin B or silibinin raman spectra. We also simulate Raman spectra of silybin B and silybin A with silver based on density functional theory (DFT) calculations .

### References:

- [1] A Solís-Gómez, RY Sato-Berrú, ME Mata-Zamora, JM Saniger, RA Guirado-López. Characterizing the properties of anticancer silibinin and silybin B complexes with UV-Vis, FT-IR, and Raman spectroscopies: A combined experimental and theoretical study. *Journal of Molecular Structure*. 1182 (2019), 109-118.
- [2] R. Y. Sato-Berrú, A. R. Vázquez-OlmosE, V. Mejía-Uriarte, et al. Synthesis of Silver Colloids with a Homemade Light Source. *Journal of Cluster Science*. 29 (2018), 719–724.
- [3] R. Mohammadinejad, Sh. Pourseyedi, A. Baghizadeh, Sh. Ranjbar, G. A. Mansoori. Synthesis of Silver Nanoparticles Using Silybum Marianum Seed Extract. *Int. J. Nanosci. Nanotechnol.*, 9 (4) (2013), 221-226.

Acknowledgement: The authors acknowledge the support of the IN-111216 and IN-102917 PAPIIT-UNAM project and CONACYT 2014-Fronteras de la Ciencia 2016 project.

## **Decoration of graphene oxide (GO) with metallic nanoparticles (NPs) for silybin detection at low power laser**

A. Solís-Gómez, J. G. Bañuelos-Muñetón, J. M. Saniger

Universidad Nacional Autónoma de México, Instituto de Ciencias Aplicadas y Tecnología, Mexico city, Mexico

Photodynamic therapy is one of the proposed ways to increase temperature locally in malicious cells. However, the low power used in the photodynamic therapy lasers require, typically, metallic particles to aide absorbing the heat. Another obstacle is the possible toxicity of the metallic particles. Silybin is an antihepatotoxic polyphenolic substance isolated from the milk thistle plant, used for the treatment for several diseases. Carbon and its allotropic forms are subject to a longstanding tradition in research. All these exhibits interesting open scientific questions and technological challenge to tackle. The present investigation proposed a facile method for the decoration of graphene oxide (GO) with Gold (Au) and Silver (Ag) nanoparticles (NPs). The hybrid materials (Au-GO, Ag-GO) were prepared by in-situ reduction of  $\text{HAuCl}_4$  and  $\text{AgNO}_3$  into graphene oxide (GO) dispersions using sodium borohydride and sodium citrate as reductant; the growth of gold and silver nanoparticles was induced by the joint effect of light and chemical reductor. The resulting hybrid materials were characterized with UV-Vis, Raman spectroscopies and Atomic Force microscopy. The characterizations revels the nanoparticles growth were induced by the joint effect of light and chemical reductor. SERS substrates were used to detect silybin at low concentration using low power laser.

### **Acknowledgment:**

The authors acknowledge the support of the IN-111216 and IN-102917 PAPIIT-UNAM project and CONACYT 2014-Fronteras de la Ciencia 2016 project

## **Raman imaging as complementary technique for the study of molecular self-assembly on surfaces**

M. L. Para<sup>1</sup>, O. E. Linarez Pérez<sup>2</sup>, M. López Teijelo<sup>3</sup>

<sup>1</sup>INFIQC-CONICET-UNC, Departamento de Físicoquímica, Facultad de Ciencias Químicas, Universidad Nacional de Córdoba, Córdoba, Argentina, <sup>2</sup>INFIQC-CONICET-UNC, Departamento de Físicoquímica. Facultad de Ciencias Químicas. Universidad Nacional de Córdoba, Córdoba, Argentina, <sup>3</sup>Universidad Nacional de Córdoba, Departamento de Físicoquímica, Facultad de Ciencias Químicas., Córdoba, Argentina

The self-assembled monolayers (SAMs) are bidimensional arrays spontaneously generated onto the surface of different substrates in contact with molecules containing specific anchorage groups. Among usually employed adsorbates, alkanethiols and aromatic molecules present special characteristics that confer interesting properties to the surface for applications in electrochemistry, molecular electronics and biochemistry. In the case of aromatic molecules,  $\pi$ - $\pi$  attractive interactions between neighbor molecules also appear, favoring formation of domains with an ordered packing, which are commensurate to and with the same symmetry of the surface. Since the layers are often discontinuous, it is important to know the distribution of the exposed areas that remain unchanged. Then, the uncovered areas may present electroactive response and can be easily evaluated by electrochemical techniques.

In this work, we use Raman spectroscopy as a complementary technique for the study of isonicotinic acid (INA) adsorption process on gold surfaces. Raman results allow obtaining conclusive evidences of both the study of chemical interaction between adsorbate and surface as well as monitoring the surface coverage evolution by means of 2D mapping.

## Magnetic graphene oxide-based composite: An attractive approach towards molecular sensing

D. M. Arciniegas Jaimes<sup>1</sup>, P. Márquez<sup>2</sup>, A. Ovalle<sup>2</sup>, J. Escrig<sup>2</sup>, O. Linarez Pérez<sup>3</sup>, N. Bajales<sup>4</sup>  
<sup>1</sup>IFEG, CONICET, Ciencia de Materiales, Córdoba, Argentina, <sup>2</sup>Universidad de Santiago de Chile, Department of Physics, Santiago de Chile, Chile, <sup>3</sup>CONICET, INFIQC - FCQ, UNC, Departamento de Físicoquímica, Córdoba, Argentina, <sup>4</sup>IFEG, CONICET - FaMAF, UNC, Ciencia de Materiales, Córdoba, Argentina

Magnetic nanostructures may be composited with graphene-like materials to obtain enhanced multiplexed attributes. A current low-cost source of easy access and non-toxic nature, is focused on graphene oxide (GO). Epoxide and OH functional groups make the GO hydrophilic and dispersible in aqueous media with long-lasting stability. Moreover, GO behaves as insulator or semiconductor, depending on the oxidation degree. One of the most recent applications of GO is its use in molecular sensors, since it provides large surface area and the presence of functional groups on the surface which serves as anchorage points to pin molecules. Thus, functionalization of GO with metal or metal oxide nanoparticles, giving rise to multifunctional composites, can enhance the electrochemical sensing properties. In this work, permalloy nanowires (Py NWs)/GO composite was obtained by decorating thick GO multilayered films with ~30 nm in diameter and 1  $\mu\text{m}$  long Py NWs, intercalated with aleatory distribution among the GO layers. Py NWs were synthesized by electrodeposition inside alumina templates, and the carbonaceous matrix was prepared from commercial GO by applying sonication and sequential deposition steps. SEM images showed that the GO film surface is decorated with several decoupled Py nanowires arrays; most of them oriented parallel to the GO surface plane and probably overlapped among some GO layers. This indicates that Py agglomerates are located around the edges of the multi-layered GO thick films and also intercalated among their layers, which is probably due to the anchorage of Py NWs to GO layers promoted by the functional groups in GO. SAXS measurements provided additional evidence for the distribution of particle sizes in the composite. An exhaustive comparative analysis between Raman spectra of GO and Py NWs/GO composite indicates that the chemical nature of GO in the composite is preserved. On the other hand, the bands expected for the Py NWs are not resolved in the corresponding Raman spectrum when it is acquired from 250 to 3250  $\text{cm}^{-1}$ . This is probably due to the low density of decoupled nanowires in the Py sample. Identification of relevant bands were positioned around 445 and 613  $\text{cm}^{-1}$ , and have been associated to the Ni–O and Fe–O, respectively. This result suggests a certain degree of oxidation of the NWs in the sample that was also supported by XPS measurements. Thus, Py NWs/GO composite arises as an attractive potential material towards molecular sensing.

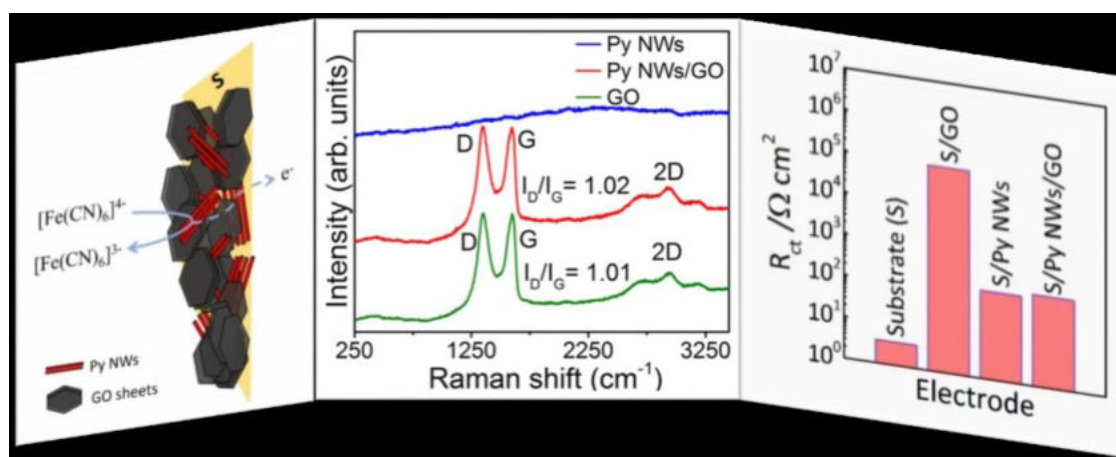


Figure: (left) Py NWs/GO sketch, (center) Raman spectra of GO (green), Py NWs/GO composite (red), and Py NWs (blue), (right) Charge-transfer resistance of the different electrodes.

## COMPARATIVE RAMAN SPECTROSCOPY STUDIES OF SOME CARBONACEOUS MATERIALS

C. Pachiu

IMT Bucharest, L9, Bucuresti, Romania

**Graphene** is a carbonaceous family member with a single atomic layer of graphite, one of the most investigated materials because of its excellent mechanical, thermal, optical and electronic properties.

**Nanocrystalline graphite/graphene** (NCG) and **vertical graphene** (VG) cannot reach the high performance of large-area graphene but these possess the attractive properties induced by its oriented arrangement.

*This work presents a systematic study of the structural characterization by Raman spectroscopy of some carbonaceous material with graphene-like structure, such as single layer graphene, vertical graphene and nanocrystalline graphite/graphene.* For Raman spectroscopy, a high-resolution Scanning Near-Field Optical Microscope fitted with a Raman Module (Witec Alpha 300S) with 532 nm wavelength diode-pumped solid-state laser and maximum power 145 mW. The incident laser beam (a 1.0  $\mu\text{m}$  spot-size) was focused with a 100 x long working distance microscope objective and the spectra were collected with an exposure time of 20s accumulation and 600 grooves/mm grating. There are different ways in which carbonaceous materials can be created, but by far the most popular way at this moment in time is by using a process called chemical vapour deposition. In this study, the materials were grown by Plasma enhanced chemical vapor deposition (PECVD) - thermal method in  $\text{CH}_4:\text{H}_2$  atmosphere at an optimized temperature on Cu or  $\text{SiO}_2/\text{Si}$  substrates. From the integrated intensities of the disorder-induced D and G Raman bands ID/IG ratio for each carbonaceous material, the lateral crystallite size of graphitic domains, number of graphene layer and defect density was determined. In particular, the parameters play a decisive role in the quality determination of graphene-based materials and applications such as energy storage, environmental remediation, sensors and biomedical.

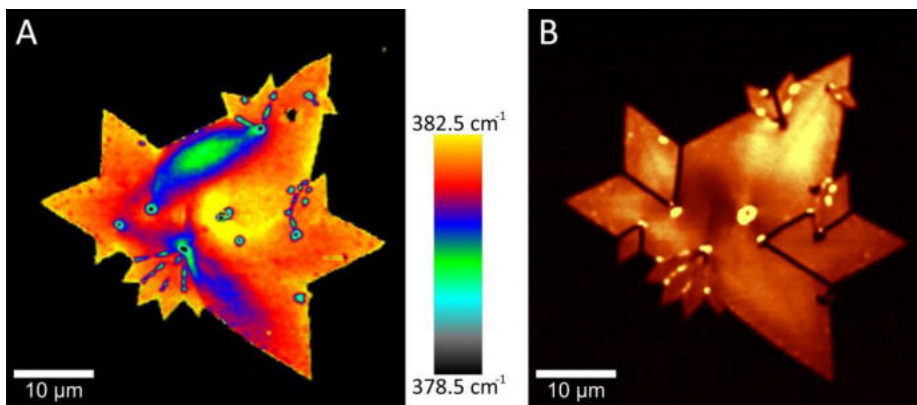
# Correlative Imaging Applications

## Correlative Raman imaging characterizes crystal properties of 2D materials

U. Schmidt<sup>1</sup>, S. Gomes da Costa<sup>1</sup>, E. Kallis<sup>1</sup>, H. Hu<sup>2</sup>, T. Dieing<sup>1</sup>, O. Hollricher<sup>1</sup>

<sup>1</sup>WITec GmbH, Ulm, Germany, <sup>2</sup>WITec Beijing Representative Office, Beijing, China

Due to their unique optical and electronic properties, two-dimensional (2D) materials have great potential for application in optoelectronic devices. Diverse crystal properties such as the number of layers and growth defects influence the optical and electronic properties of the 2D materials. Research, development and quality control thus require powerful and non-destructive imaging techniques for monitoring these crystal properties and to evaluate synthesis processes. To comprehensively characterize the 2D material, it is advantageous to combine several imaging techniques. Here, we present correlative Raman imaging as a versatile tool for investigating prominent examples of 2D materials, namely graphene and the transition metal dichalcogenides (TMDs) molybdenum disulfide ( $\text{MoS}_2$ ) and tungsten disulfide ( $\text{WS}_2$ ). In combination with imaging techniques such as second harmonic generation (SHG), photoluminescence (PL), atomic force microscopy (AFM) or scanning electron microscopy (SEM), Raman imaging is able to provide a thorough characterization of the 2D materials. Crystal properties and features such as grain boundaries, surface structure, layer number, defect density, doping and strain fields can thus be identified and visualized.



Correlative Raman and SHG imaging of mono-layer  $\text{MoS}_2$ . The Raman image (A) shows the frequency of the  $E_{2g}$  mode, indicating strain fields. The SHG intensity image (B) reveals grain boundaries (low intensity).

## **Detecting Nanoplastic Particles using Correlative Microscopy**

R. Schmidt<sup>1</sup>, H. Fitzek<sup>2</sup>, M. Nachtnebel<sup>2</sup>, A. Zankel<sup>1</sup>, H. Schröttner<sup>1</sup>, M. Dienstleder<sup>3</sup>, S. Mertschnigg<sup>4</sup>, M. Poteser<sup>5</sup>, H.-P. Hutter<sup>5</sup>, W. Eppel<sup>6</sup>

<sup>1</sup>Institute of Electron Microscopy and Nanoanalysis (FELMI), Technische Universität, Graz, Austria, <sup>2</sup>Centre for Electron Microscopy, Graz, Austria, <sup>3</sup>Center for Electron Microscopy Graz, Graz, Austria, <sup>4</sup>Institute of Electron Microscopy and Nanoanalysis (FELMI), Graz, Austria, <sup>5</sup>Centre for Public Health, Medical University Vienna, Vienna, Austria, <sup>6</sup>Medical University of Vienna, Department of Obstetrics and Gynecology, Vienna, Austria

Nowadays “microplastics” (MPs) is an already well-known term and micro-sized particles are increasingly found in several consumer products [1]. Moreover, effects of micro- and nanoplastics (NPs) on human health have been investigated and discussed [2]. In this study, the focus is pointed to MPs smaller than 1 µm, with a specific focus on particles in the scale of a couple of 100 nm, which are referred here as NPs. A correlative approach between scanning electron microscopy (SEM, high resolution) and Raman microscopy (chemical identification) was tested to meet the challenges of finding and identifying these small particles. For this purpose standardized polystyrene (PS) beads were mixed into various environments in different concentrations, ranging from ideal (distilled water) to realistic (sea salt, human amniotic fluid), to proof the detection limit of NPs with the so called RISE (Raman Imaging and Scanning Electron microscopy) system [3]. Promising results exhibit detection limits of  $2 \cdot 10^{-3}$  µg/L (distilled water), 20 µg/L (sea salt) and 200 µg/L (human amniotic fluid).

[1] M. E. Iñiguez, J. A. Conesa, and A. Fullana, “Microplastics in Spanish Table Salt,” *Sci. Rep.*, vol. 7, no. 1, p. 8620, Dec. 2017, doi: 10.1038/s41598-017-09128-x.

[2] E. Sazakli and M. Leotsinidis, “Possible effects of microplastics on human health,” in *Microplastics in Water and Wastewater*, IWA Publishing, 2019, pp. 177–190.

[3] R. Schmidt, H. Fitzek, M. Nachtnebel, C. Mayrhofer, H. Schroettner, and A. Zankel, “The Combination of Electron Microscopy, Raman Microscopy and Energy Dispersive X-Ray Spectroscopy for the Investigation of Polymeric Materials,” *Macromol. Symp.*, vol. 384, no. 1, pp. 1–10, 2019, doi: 10.1002/masy.201800237.

## **Correlating SEM and Raman Imaging of Nucleopore Filter Sampled Nanofibers**

A. Meyer-Plath, J. Schumann, S. Plitzko

Federal Institute for Occupational Safety and Health (BAuA), FG. 4.5, Berlin, Germany

In the light of the “Global Asbestos Disaster” [1], human exposure to high concentrations of respirable biopersistent fibers must be controlled. Reports on the asbestos-like pathogenic potential of rigid and biodurable nanofibers of multi-walled carbon nanotube type [2,3] make it necessary to determine concentrations of airborne nanofibers at a level of 10,000 fibers/m<sup>3</sup>. BAuA develops such techniques based on sampling aerosols on nucleopore filter membranes, followed by SEM imaging. For every nanofiber recognized and localized on an SEM image, Raman analysis is mandatory to distinguish natural fibers like cellulose from man-made biodurable fibers. The high workload on SE and Raman microscopes motivated to use not an SEM-integrated Raman but two independent instruments to parallelize the analysis. We have developed a method to automatically position filters in the Raman with an accuracy better than 100 nm to address and Raman image all candidate fibers of a sample. This enables to check compliance with recommended nanofiber exposure limits [4].

Using the Hitachi and WITec software APIs, a software was developed to control both the SU8230 SE and Apyron Raman microscopes. The software first automatically acquires focused SEM images at statistically random locations of a position-calibrated filter. Its track-etched pores of 400 nm diameter can also be resolved in our Apyron using a 100X objective. Convolution of both images with a “standard pore” kernel results in pore position images that allow correlating the pore constellation in the vicinity of a nanoscale object to analyze.

This pattern matching approach allows improving the initial filter positioning accuracy of about 5 µm to better than 100 nm. This way, even optically non-resolvable objects can be localized.

WITec’s microscope controller API gives full access to all necessary hardware features (except stage acceleration limits) to achieve not only image analysis and stage control but to implement even complex analysis workflows.

1. Furuya et al. DOI 10.3390/ijerph15051000
2. Rittinghausen et al. DOI 10.1186/s12989-014-0059-z
3. Broßell et al. in DOI 10.20850/9781716632426
4. <https://www.baua.de/EN/Service/Legislative-texts-and-technical-rules/Rules/TRGS/TRGS-527.html>

## Q-switched Nd:YAG laser on dental enamel with photoabsorber: a confocal Raman pilot study

P. Castro<sup>1</sup>, D. Pereira<sup>1</sup>, P. Ana<sup>2</sup>, C. Matos<sup>3</sup>, D. Zezell<sup>1</sup>

<sup>1</sup>Nuclear and Energy Research Institute, Center for Lasers and Applications, Sao Paulo, Brazil, <sup>2</sup>Engineering Modelling and Applied Social Sciences Center, Santo Andre, Brazil, <sup>3</sup>MackGraphe - Graphene and Nanomaterials Research Center, Sao Paulo, Brazil

Nd:YAG lasers emitting  $\lambda = 1064$  nm at microsecond and nanosecond pulses are alternatives to prevent dental caries and erosion in clinics. This wavelength allows most of photons to penetrate deep in the hard tissue due to low absorption of hydroxyapatite in the region. It is necessary to use photoabsorbers so most of photons are absorbed in the surface of the tissue preventing dental pulp necrosis. Currently the coal paste is used as a photoabsorber but the irradiated tissue turns darker what implies in the patients low adherence to the treatment due to aesthetic reasons. [1,2]. Confocal Raman spectroscopy is a non-destructive optical method to obtain detailed information about molecular composition of biological structures in depth. The most prominent feature of Confocal Raman spectroscopy is the reliable capability to provide the biomolecular data with no use of ionizing radiation to penetrate in the sample. This work aims to characterize the dental enamel irradiated with Nd:YAG laser with nanoseconds pulses, in order to describe the depth related changes promoted in the enamel, by the heat generated due to laser irradiation. For these measurements, 30 bovine enamel blocks of  $8 \text{ mm}^2$ , were randomized into 3 groups: G1 – enamel untreated; G2 – enamel irradiated with Nd:YAG nanopulsed laser (1064 nm, 4 W;  $1,05 \text{ J/cm}^2$ ; 5 ns 20 Hz, Brilliant, Quantel Laser) using a coal paste as photoabsorber; G3 -enamel irradiated with Nd:YAG nanopulsed laser (same parameters as G2) using squid ink as photoabsorber. The assessments of three different depth regions of the cubic shaped samples were: region A- left corner above of the sample, region B-middle of the sample and Region C- right corner below of the sample. The intensity map of phosphate ( $950 \text{ cm}^{-1}$ ) regarding the position, were calculated [3,4] as shown in the Figure 01.

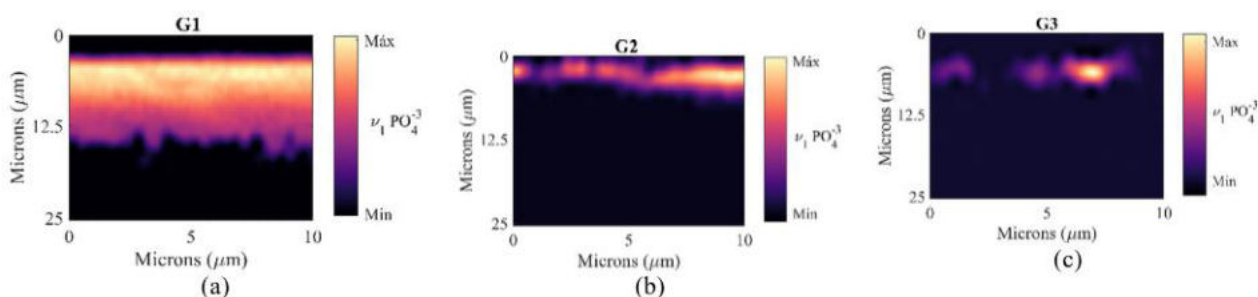


Figure 01: Phosphate intensity maps of (a) Enamel untreated - (b) Enamel with coal paste irradiated with Nd:YAG nanopulsed laser (c) Enamel with squid ink irradiated with Nd:YAG nanopulsed laser.

The comparative results in the Fig.1 demonstrated that application of coal paste associated with Nd:YAG (G2) can preserve the inorganic content better than the squid ink group (G3). These findings have crucial clinical implications in the laser protocol development and it was possible to correlate the heat penetration depth of the laser irradiation with photoabsorber using the images obtained by the confocal Raman.

## REFERENCES

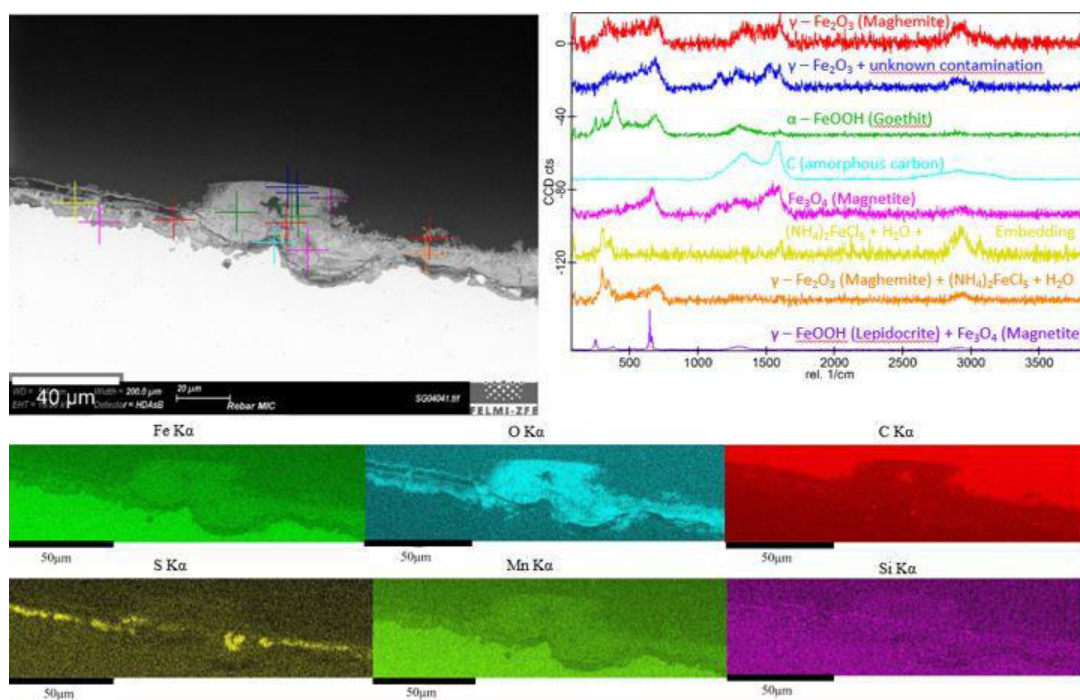
- [1] D. L. Pereira et al, Int J Mol Sciences 19, 433-447, 2018.
- [2] P. A. Ana et al, Caries Res, 46, 441-451, 2012.
- [3] J. B. Holly et al, Nat. Protocols. 11, 664–687, 2016.
- [4] H. C. Charles et al, Nat. Photonics 8, 627-634, 2014.

## Microbiologically influenced corrosion (MIC) of steel – a study using correlative SEM, EDX and Raman microscopy

T. Planko<sup>1</sup>, H. Fitzek<sup>1</sup>, S. Eichinger<sup>2</sup>, J. Rattenberger<sup>1</sup>, G. Koraimann<sup>3</sup>, H. Schröttner<sup>1,4</sup>

<sup>1</sup>Graz Centre for Electron Microscopy, Graz, Austria, <sup>2</sup>Graz University of Technology, Institute of Applied Geosciences, Graz, Austria, <sup>3</sup>University of Graz, Institute of Molecular Biosciences, Graz, Austria, <sup>4</sup>Graz University of Technology, Institute of Electron Microscopy and Nanoanalysis, Graz, Austria

Microbiologically influenced corrosion (MIC) is responsible for 20% of all corrosion damage [1]. In this context, there is great interest in understanding MIC especially, since it has been shown that some microbes slow down the rate of corrosion [2], while others speed it up [3]. During experiments in the Koralm tunnel, iron-oxidizing bacteria were found, to be part of a MIC causing, microbial community. The aim of the investigations is to observe the influence of MIC on steel on the macroscopic (corrosion rates CR, pitting corrosion), and the microscopic side. A novel technique is applied for the latter, which combines Raman imaging with scanning electron microscopy (SEM) and energy dispersive X-Ray spectroscopy (EDX) (Zeiss Sigma 300 VP; Oxford X-Max 80; WITec RISE). An example of a correlative SEM-EDX-Raman (RISE) measurement is shown in the figure.



RISE-measurement: rebar-steel (bio-corroded, cross-section); Top: SEM-image with Raman positions, and Raman spectra: Maghemite, Goethite, amorphous carbon, Magnetite, Lepidocrite; Bottom: EDX-mappings: iron, oxygen, carbon, sulfur, manganese, silicon.

The result showed that the CR of those samples exposed to MIC was two to six times lower than the reference samples. This is because bacteria placed a thin layer of sulfur over the sample (see figure 1, bottom left). A sulfur layer reduces the CR by acting as a solid diffusion barrier [4].

### References:

- [1] Dubiel, M., *et al.* Appl. Environ. Microbiol. 68.3 (2002), p. 1440-1445.
- [2] Javed, M. A., *et al.* International Biodeterioration & Biodegradation 125 (2017), p. 73-85.
- [3] Wade, S. A., *et al.* International Biodeterioration & Biodegradation 121 (2017), p. 97-106.
- [4] ZHENG, Yougui, *et al.* CORROSION/2015, 2015, p. 5933.

The authors gratefully acknowledge funding from the Austrian Cooperative Research (ACR) under the ACR-Project: "KorronNet": Avoidance of selective corrosion

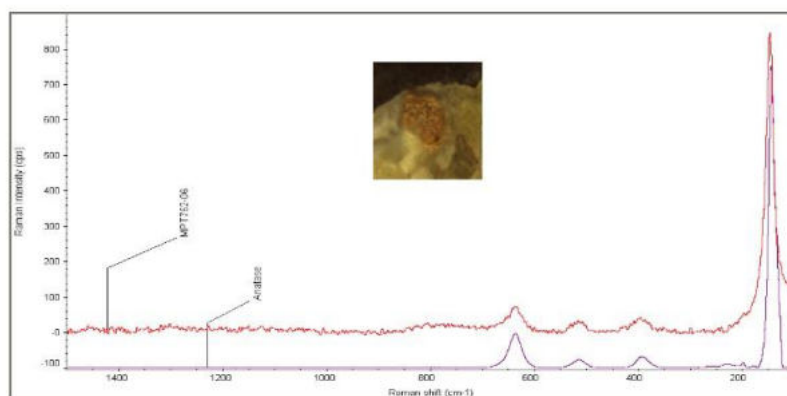
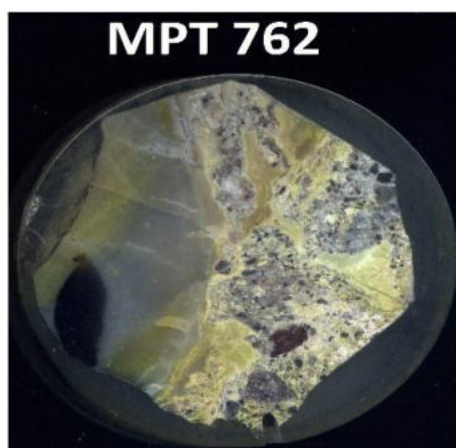
# **Environmental and Geoscience**

## Application of Raman microscopy to the study of the mineralogical composition of pyroclastic rocks from Lesvos petrified forest

A. IORDANIDIS<sup>1</sup>, J. GARCIA-GUINEA<sup>2</sup>, N. ZOUROS<sup>3</sup>, A. ASVESTA<sup>1</sup>

<sup>1</sup>University of Western Macedonia, Mineral Resources Engineering, Kozani, Greece, <sup>2</sup>Museo Nacional Ciencias Naturales, CSIC, Madrid, Spain, <sup>3</sup>University of the Aegean, Geography, Mytilene, Greece

The Lesvos Petrified Forest was formed by silicification process of plants during the Lower Miocene era, when intense volcanic activity occurred in that region. Situated in the western part of Lesvos island (NE Greece) and consisting of hundreds of standing and lying fossilized tree trunks, it is one of the most important natural heritage monuments in the world. Despite its significance, the conduction of extensive mineralogical analyses on fossil plants and their hosting pyroclastic rocks has merely commenced, providing information on the permineralization process. Sigri pyroclastic rock samples were collected within the Lesvos Petrified Forest, and four polished block sections with embedded fossil plant material were created for analytical purposes. A Thermo Scientific DXR Raman Microscope with a 780 nm laser beam was employed. The power value of the sample irradiation was ranging from 6 mW to 12 mW. The average spectral resolution in the Raman shift range of 100-3000  $\text{cm}^{-1}$  was  $5\text{cm}^{-1}$  (grating 400 lines/mm, spot size  $2\mu\text{m}$ ). Magnetite was revealed with its intensive band at  $662\text{ cm}^{-1}$ , along with anatase (titanium oxide) showing an intensive band at  $144\text{ cm}^{-1}$  and secondary bands at 396, 516 and  $637\text{ cm}^{-1}$ . Apatite with its distinct strong peak at  $965\text{ cm}^{-1}$  was also determined along with biotite from the mica group and labradorite and sanidine from the feldspars group. Pyrolusite (manganese oxide) revealed its characteristic peaks at 503 and  $573\text{ cm}^{-1}$  and lepidocrocite showed two strong peaks at 256 and  $440\text{ cm}^{-1}$  and several secondary peaks at 170, 285, 525 and  $695\text{ cm}^{-1}$ . Hematite (iron oxide) was also evident with three strong peaks at 220, 287 and  $1315\text{ cm}^{-1}$  and some weaker peaks at 402, 607 and  $651\text{ cm}^{-1}$ . Overall, the utilization of Raman micro-spectroscopy provided substantial information for the identification of the mineral assemblages comprising the pyroclastic rocks hosting the Lesvos petrified wood samples.



Polished block section of the MPT762 fossil plant/pyroclastic rock sample [left] and characteristic Raman spectra of an anatase mineral phase (red), comparing to the standard anatase mineral (purple) [right]

## **Image of microplastics and nanoplastics**

C. Fang, Z. Sobhani  
UON, Newcastle, Australia

We demonstrate that Raman imaging can be employed to visualise and identify microplastics and nanoplastics down to 100 nm, by distinguishing the laser spot, the pixel size/image resolution, the nanoplastics size/position (within a laser spot), the Raman signal intensity.

We also examine the lateral intensity distribution of the Raman signal emitted by nanoplastics (diameters ranging ~30–600 nm) within the excitation laser spot. We find that the Raman emission intensity, similar to the excitation power density distributed within a laser spot, also follows a lateral Gaussian distribution. We break down the diffraction limit of laser and cross-check multi-images simultaneously mapped at two or three characteristic peaks via either a logic-OR or a logic-AND algorithm. Thus the imaging uncertainty can be significantly reduced from a statistical point of view.

## Using Cryo-Raman spectroscopy to analyse the location and chemistry of micro-inclusions in the EastGRIP ice core

N. Stoll<sup>1</sup>, J. Eichler<sup>1</sup>, I. Weikusat<sup>1, 2</sup>, D. Dahl-Jensen<sup>3</sup>

<sup>1</sup>Alfred Wegener Institute, Helmholtz Centre for Polar and Marine Research, Geosciences, Bremerhaven, Germany,

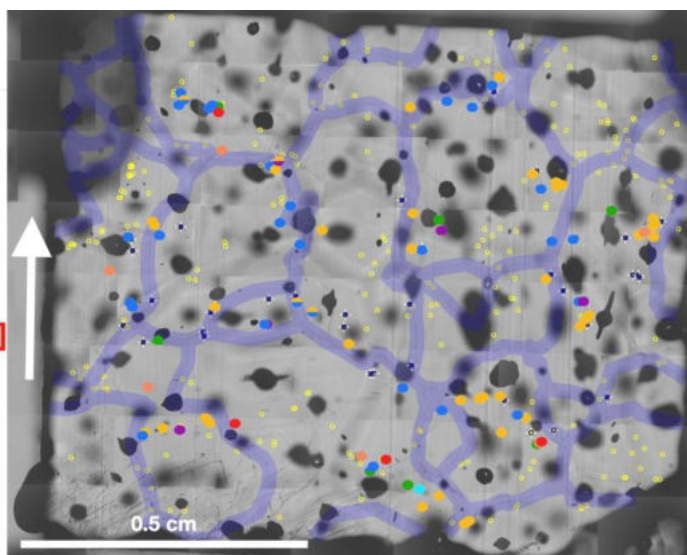
<sup>2</sup>Eberhard Karls Universität Tübingen, Geosciences, Tübingen, Germany, <sup>3</sup>Physics of Ice, Climate and Earth, Niels Bohr Institute, Copenhagen, Denmark

One of the major uncertainties regarding future sea-level rise is the physics behind the flow of ice, which significantly impacts the amount of solid ice discharge into the oceans. Various physical properties of polar ice are affected by impurities in ice, ranging from electrical conductivity to internal deformation and thus, ice flow. Our goal is to better understand the impact of impurities on the deformation of ice by analysing the *East Greenland Ice Core Project* (EastGRIP) ice core. The on-going EastGRIP drilling delivers the first deep ice core from a fast-flowing ice stream, the *Northeast Greenland Ice Stream*, enabling novel in-situ information on the flow of ice. We analysed seven samples from various depths of the first 900 m of the ice core in our cold lab (-15°C). First, we used an optical microscope to map the surface of the sample and the same area focused 500 µm below the surface. These maps allow us to locate micro-inclusions, solid impurities of µm-size, inside the ice while preserving the original microstructure and preventing contamination. Following this, a WITec alpha 300 M+ confocal cryo-Raman system with a Nd:YAG laser (532 nm) is used to analyse the chemical composition of these inclusions.

We present impurity distribution and mineralogical data from seven different depths of the EastGRIP ice core. Preliminary key findings are 1) a homogenous spatial distribution of impurities in the microstructure, 2) distinct layers of impurity-rich grains, 3) a strong relationship between identified minerals and the bulk chemistry, and 4) a diverse chemical range of micro-inclusions mainly consisting of sulfates (e.g., gypsum) and insoluble terrestrial minerals such as quartz, mica or feldspar.

**EGRIP 504\_3**  
**- 277m**

Sulfate (X)SO<sub>4</sub>  
Quartz SiO<sub>2</sub>  
Gypsum  
Ca(SO<sub>4</sub>)\*H<sub>2</sub>O  
Mica  
K/Al/[AlSi<sub>3</sub>O<sub>10</sub>(OH)<sub>2</sub>]  
Feldspar  
Ca,K[Al,Si]<sub>4</sub>O<sub>8</sub>  
Carbonous C  
Hematite  
Fe<sub>2</sub>O<sub>3</sub>



Located impurities in an ice core sample from 277 m of depth. Colored dots represent identified compounds, blue thick lines indicate grain boundaries at the sample surface. The arrow points towards the surface of the ice sheet.

## Raman mapping of complex mineral assemblages: application on pegmatitic phosphates sequences

F. Prado Araujo, N. Hulsbosch, P. Muechez  
KU Leuven, Leuven, Belgium

Phosphate minerals form an important part of many geological and biological systems. In geological systems, phosphates occur nearly in all rock types, being particularly abundant in sedimentary (e.g. phosphorite) and magmatic rocks. In the latter, pegmatites are highlighted for their vast and exceptionally rich phosphate mineralogy. Changes in physico-chemical conditions during crystallization of phosphates are reflected on the sequence of formation for these minerals, termed paragenesis. Raman imaging is able to detect those mineralogical changes in complex assemblages with high spatial resolution, successfully determining the paragenesis. Raman spectroscopy is more advantageous than conventional methods because it requires little sample preparation, it is non-destructive, and is capable of identifying hydrated minerals and phases composed of light elements (e.g. H, Li). This study applies state-of-the-art Raman imaging techniques to define the formation sequence of complex mineral assemblages in the Buranga rare-metal pegmatite, a P-Li-Nb-Ta-rich magmatic rock from Western Rwanda. The Buranga dyke was chosen for the development of the Raman mapping methodology of complex mineral assemblages because it hosts more than 50 phosphate species, often with intergrowth or replacement textures. Our results show the replacement of amblygonite  $[\text{LiAl}(\text{PO}_4)\text{F}]$  by montebrasite  $[\text{LiAl}(\text{PO}_4)\text{OH}]$ . Mapping of the OH-stretching peak position around  $3360\text{ cm}^{-1}$  and the peak width identifies the mineral phases, illustrates their spatial relations, and allows to estimate the distribution of fluorine within the sample. We also investigate the replacement textures of phosphate minerals in a complex assemblage. Each observed phase has unique spectral features that allow their identification and classification in the Raman maps. The sequence trolleite  $[\text{Al}_4(\text{PO}_4)_3(\text{OH})_3]$  + rosemaryite  $[\text{Na}(\text{Mn}^{2+}, \text{Fe}^{2+})\text{Fe}^{3+}\text{Al}(\text{PO}_4)_3]$   $\rightarrow$  lazulite-scorzalite  $[(\text{Mg}, \text{Fe})\text{Al}_2(\text{PO}_4)_2(\text{OH})_2]$   $\rightarrow$  samuelsonite  $[\text{Ca}_9(\text{Fe}, \text{Mn})_4\text{Al}_2(\text{PO}_4)_{10}(\text{OH})_2]$   $\rightarrow$  wardite  $[\text{NaAl}_3(\text{PO}_4)_2(\text{OH})_4 \cdot 2\text{H}_2\text{O}]$  is proposed for this assemblage. Raman maps show that the Buranga pegmatite experienced a progressive hydration process during cooling, followed by internal remobilization of elements, such as F, Li, Na, and Ca. Our data confirm that phosphates in complex mineral assemblages can (1) be straightforwardly analyzed by Raman images, (2) record the evolution of the magmatic host rock, and (3) be used as proxies for pegmatite formation.

## Transport of diesel soot particles in structured and homogenized soil visualized by hyperspectral imaging and confocal Raman microscopy

M. Ortner<sup>1</sup>, H. Buddenbaum<sup>2</sup>, S. Thiele-Bruhn<sup>1</sup>

<sup>1</sup>University Trier / Regional and Environmental Sciences, Soil Science, Trier, Germany, <sup>2</sup>University Trier / Regional and Environmental Sciences, Environmental Remote Sensing and Geoinformatics, Trier, Germany

Each year diesel motor-vehicle exhausts produce about 1.8 g soot/km along the roadsides in Germany. Containing a high amount of hydrophobic pollutants, a transport of soot particles in soil could lead to contamination of water and of soil itself. Knowledge about the retardation or transport in soil of deposited soot are largely missing. This study aimed to elucidate whether deposited soot is accumulated on the soil surface or whether it is transported, possibly through coarse soil pores, downwards.

To determine soot mobility in soil, diesel soot was applied on top of structured and unstructured soil, respectively, contained in columns with a length of 12 cm and a diameter of 4.70 cm. A constant water flow was established for one month to enable soot particles to move downwards. Subsequently, soil columns were cut open and air-dried for further analysis. Hyperspectral imaging was used to identify clusters of soot particles in the soil columns. To determine the depth distribution of soot particles, the hyperspectral data was analyzed by using Maximum Likelihood Classification (MLC), Spectral Angle Mapper and autoPartial Least Squares Regression (aPLSR). The received hyperspectral images of soot concentration along the depth gradients were used to identify soot by using Confocal Raman Microscopy (WITec alpha300 R). Hyperspectral data enabled to separate pixels into several clusters according to the concentration of soot on the soil, while Raman microscopy was able to unequivocally distinguish soot from soil organic matter or blackish minerals. Single soot particles were identified in structured as well as in unstructured soil columns. The concentration of soot particles declined with increasing soil depth, while most soot particles remained on the top of the soil columns. Those soot particles that were identified deeper in the soil were mostly found alongside of larger cracks and pores of the columns indicating their function as preferential flowpaths for particles in soils. Particularly in structured soil columns more soot particles were found in deeper soil, while in the unstructured soil columns less soot particles were translocated but remained on the top of the soil. The combination of hyperspectral imaging with confocal Raman microscopy effectively enables to localize, quantify and identify soot in heterogeneous environmental samples such as soils.

## **Detection of different microplastic materials in soil by using confocal Raman microscopy**

M. Ortner<sup>1</sup>, A. Stablo<sup>2</sup>, S. Thiele-Bruhn<sup>1</sup>

<sup>1</sup>University Trier / Regional and Environmental Sciences, Soil Science, Trier, Germany, <sup>2</sup>University Trier / Regional and Environmental Sciences, Soil Science, Trier, Germany

Plastic particles are distributed worldwide in every ecosystem. For soils there are several possible input pathways such as the application of manure, plastic mulching or by atmospheric deposition. With decreasing particle size, the identification gets more difficult. Actually, several approaches are tested for quantitative and qualitative analysis of microplastic (MP) in soil. Physical and chemical methods are highly time consuming, cost intensive and destructive while methods using optical or spectral approaches such as microscopy, FTIR and – investigated in this study – Raman are less cost intensive and non-destructive.

Aims of this study were 1) to prove the suitability of confocal Raman microscopy to determine MP in soil and 2) to show whether biofouling or staining with mineral particles masks MP, which would be a kinetic process occurring in moist soil.

Different MP materials (PA, PP) were added in selected contents (1%, 2%, 5% w/w) to sieved air-dried soil. Samples were analyzed without further treatment. A second batch of samples was spiked with 5% MP, biologically reactivated by rewetting, and stored at 20°C for up to eight weeks. Water losses were repeatedly compensated to keep a constant soil moisture. In order to obtain a time series, samples were taken biweekly for further analysis. From each sample a randomly selected surface area was analyzed with confocal Raman microscopy (WITec alpha300 R) using a 532 nm laser. For identification of MP particles in the samples large area scan was done, covering a surface of 1000 µm × 1000 µm. Recorded spectra were treated by using background subtraction and Savitzky-Golay smoothing. Afterwards spectra were clustered using k-means algorithm allowing an identification of the applied microplastic materials.

Characterization of all MP materials was successful for all recorded spectra. Also, analysis of dry samples allowed an identification of different contents of MP particles of each plastic material in soil. Numbers of pixels identified as MP particles closely correlated with the spiking content of MP ( $R^2 = 0.77-0.99$ ). Yet, time series showed a decrease of determined MP particles from 27% after two weeks down to 3% after eight weeks.

It is concluded that Raman microscopy is a suitable technique for fast and efficient identification and quantification of MP particles in soil. However, in bioactive, moist soil recovery of MP is increasingly inhibited, most likely due to the formation of surface coatings.

## Raman spectroscopy at pressures exceeding 10 000 atm

D. Kurzydłowski<sup>1</sup>, J. Rogoża<sup>2</sup>, T. Chumak<sup>1</sup>

<sup>1</sup>Cardinal Stefan Wyszyński University in Warsaw, Faculty of Mathematics and Natural Sciences, Warsaw, Poland,

<sup>2</sup>University of Warsaw, Faculty of Physics, Warsaw, Poland

Pressures used in laboratories and industry rarely exceed 300 atm ( $\approx 0,03$  GPa). However due to the development of new measurement techniques, in particular the diamond anvil cell (DAC), it is now possible to probe *in situ* materials at pressures exceeding 1 GPa ( $\approx 10\,000$  atm), and even reaching 400 GPa ( $\approx 4 \cdot 10^6$  atm). Experiments performed at high pressure enable observation of many intriguing phenomena, such as the transformation of nitrogen into a polymeric structure resembling that of diamond.<sup>1</sup>

Here we present investigation into the high-pressure phase transitions of simple solids, including dichloromethane ( $\text{CH}_2\text{Cl}_2$ ), chloroform ( $\text{CHCl}_3$ ), and inorganic fluorides ( $\text{ZnF}_2$ ,  $\text{AuF}_3$ ) up to pressures of 45 GPa ( $\approx 450\,000$  atm). By performing Raman scattering measurements we were able to monitor the evolution of the Raman-active vibrations as a function of pressure. Comparing information on the Raman band positions and intensities with results of *ab initio* solid-state calculations enabled us to assign the evolution of the crystal structure, and phase transition sequence in these systems.<sup>2,3</sup>

An often overlooked aspect of high-pressure experiments is the homogeneity and purity of the sample. This is particularly important given the small dimensions of the DAC chamber (of an order of 100  $\mu\text{m}$ ). Thanks to the high confocality and sensitivity of our Raman microscope (Witec Alpha 300) we were able to perform Raman mapping of samples enclosed in the DAC with  $\mu\text{m}$  resolution, even at high pressures (Figure 1).

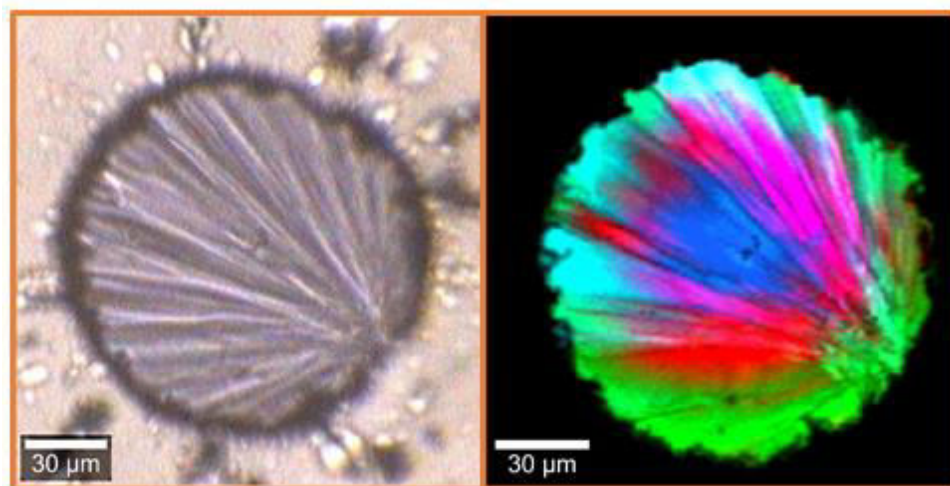


Figure 1. Photograph of solid dichloromethane compressed in a DAC (left) together with the Raman map of the sample (right). Color coding indicates different crystallite regions.

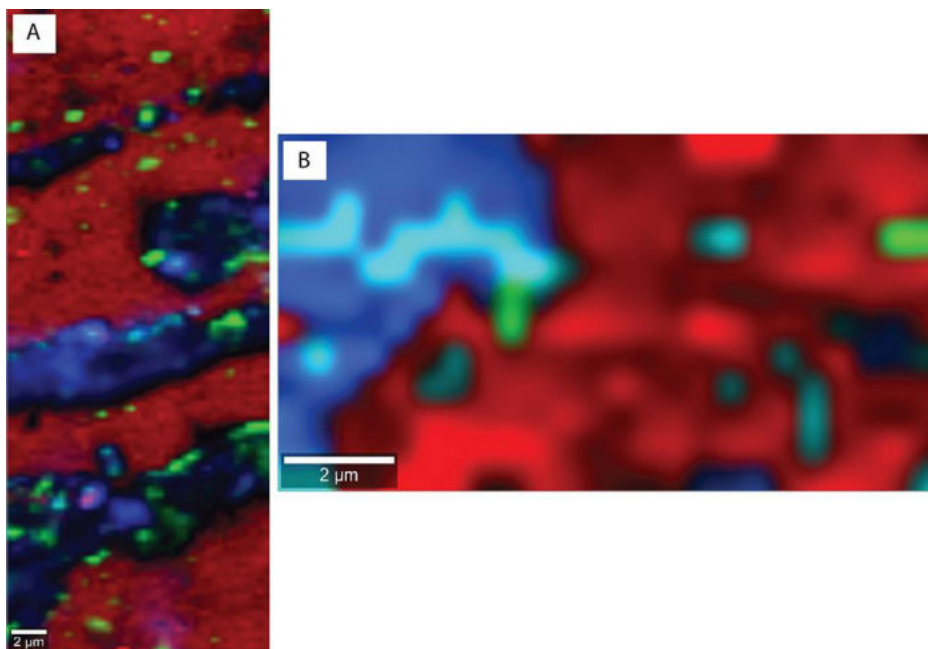
### References

1. M. I. Eremets, et al., *Nat. Mater.* 2004, **3**, 558.
2. D. Kurzydłowski, et al. *Inorg. Chem.* 2020, **59**, 2584.
3. D. Kurzydłowski, et al. *Chem. Commun.* 2020, **56**, 4902.

## Determining the Provenance of Planetary Analogs with Spatially Resolved Micro Raman Imaging of Nanocrystalline Minerals

D. Bower<sup>1</sup>, A. Steele<sup>2</sup>, M. Fries<sup>3</sup>

<sup>1</sup>University of Maryland College Park, NASA Goddard Space Flight Center, Greenbelt, United States, <sup>2</sup>Carnegie Institution for Science, Washington, DC, United States, <sup>3</sup>NASA Johnson Space Center, Houston, TX, United States



Raman maps: (A) 3.5 Ga chert with a combination of disseminated (green) carbon with layers of (blue) anatase (TiO<sub>2</sub>) in (red) quartz; (B) Recent lava with dominant minerals pyroxene (red) and plagioclase (blue & teal), and trace anatase (green).

Geologic deposits on Earth and other planetary bodies undergo several iterations of geochemical change over time resulting in compositional differences that can obscure the origins of those deposits. Our ability to reconstruct habitable environments and their evolution on other planetary bodies relies on the accurate characterization of surface deposits. In particular, the origins of both terrestrial and planetary deposits may be recorded in the mineral assemblages as barely discernible nanocrystalline phases. Micro Raman imaging facilitates the identification of nanocrystalline materials (grain size  $\leq 1$   $\mu\text{m}$ ) and their spatial relationships with micro-scale minerals for a comprehensive characterization. For many older deposits, nanocrystalline phases occur as inclusions within or along the edges of larger mineral grains. In younger or recent deposits, the nanocrystalline phases may be ephemeral and more difficult to detect. Here we explore some of the applications in which the ability to identify nanocrystalline minerals results in more robust interpretations of the rock record providing a path forward for planetary exploration using Raman spectroscopy.

## **CL and Raman imaging of metamorphic and kimberlitic diamonds**

A. KORSAKOV, D. Mikhailenko  
IGM SB RAS, NOVOSIBIRSK, Russian Federation

Cathodoluminescence image is most common tool for recovery internal morphology and growth history of diamond crystals. But there are several disadvantages of this very useful technique. First of all diamond crystal need to be polished to the central plane and at least half of the diamond crystal and the information, containing in this part, are lost during sample preparation. Our previous study reveal that confocal Raman imaging could be potentially a very good alternative of CL imaging in mineralogical study. In this study we focus on CL and Raman imaging of the Kokchetav metamorphic and Yakitiyan kimberlitic diamonds. A WITec Apyron (Automated Confocal Raman system) was equipped with a 488 nm and 635 nm lasers fiber coupled to the instrument. A 100× (NA 0.9 air) objective was used for excitation and detection. In all measurements, the laser with a power of approximately 50 mW was employed. Micro-cathodoluminescence (SEM-CL) analyses of microdiamonds were performed using a scanning electron microscope LEO 1430 VP (Carl Zeiss) equipped with a CL spectrometer. The accelerating voltage for each analysis was 20 kV. The polished microdiamonds exposed on the surface of the thin sections were analyzed. The diamond shows a strong change in the position of the diamond Raman line as well as the width of this line, which could be found both in the XY and in the YZ scan. Raman images are identical with the CL images, but in contrast to CL almost no sample preparation is required for the Raman imaging, which can be done at different depth of the diamond crystal and without any destruction of the inclusions and host-mineral. Thus Raman imaging are powerful and non destructive technique for recovery growth history and internal morphology of the diamond crystals. This study was supported by the Russian Science Foundation (Grant 18-17-00186).

**Life Sciences, Biomedical and  
Pharma Research**

### Three-Dimensional Spectroscopic Chemical Imaging of Pharmaceutical Tablets

H. Carruthers<sup>1,2</sup>, D. Clark<sup>2</sup>, F. Clarke<sup>2</sup>, K. Faulds<sup>1</sup>, D. Graham<sup>1</sup>

<sup>1</sup>University of Strathclyde, Glasgow, United Kingdom, <sup>2</sup>Pfizer UK, Sandwich, United Kingdom

Pharmaceutical tablets are the most widely used solid dosage form for delivering therapeutic agents. There are knowledge gaps in current pharmaceutical manufacturing processes; particularly those related to the relationship of components in the formulation, processing conditions and the final product characteristics. By providing a means of visualising the microstructure of a tablet matrix these areas may be better understood. There are several techniques that can generate high resolution chemical images of the component distribution within a tablet system but generally cannot go beyond an exposed surface layer. Three-dimensional imaging has been explored by using a Raman microscope to obtain a depth profile of a sample, however, this is typically less than 50 microns. The particle size of common excipients and active ingredients often exceed this depth range making it unsuitable for pharmaceutical products. Instead, this study explores an alternative method to obtain three-dimensional images of a sample using Raman and near-infrared chemical imaging. This involves stacking two-dimensional chemical images obtained at different penetration depths by physically milling the sample and may hold the key to improved fundamental understanding of solid dosage forms. This investigation has also assessed the differences in the chemical images obtained by Raman and near-infrared chemical imaging. Both techniques are closely related tools for characterising the chemical composition of a sample. Scanning electron microscopy with energy dispersive X-ray microanalysis were employed as alternative imaging techniques to evaluate which spectroscopic imaging method provided the most comparable and therefore representative image of the sample.

## Tracking heavy water incorporated confocal Raman spectroscopy for evaluating the effects of PEGylated emulsifiers on skin barrier

Y. Liu, D. Lunter

Tuebingen University, Pharmaceutical Technology, Tuebingen, Germany

The class of PEGylated emulsifiers finds broad application in the pharmaceutical and cosmetic industry. With larger use, their irritation potential and diverse effects on skin have caught our attention. We target on one of the categories of polyethylene glycol (PEG) alkyl ethers with different lipophilic and hydrophilic chain length and aim to comprehensively examine their effects on the skin. We focus on finding their interactions with skin lipid components and try to summarise the potential rules for their further appropriate selection in skin research. With these clear goals, confocal Raman spectroscopy (CRS) was employed for measurements of skin spectra in-depth and imaging. A unique probe of heavy water ( $D_2O$ ) was incorporated which can be tracked percutaneously and simultaneously monitor the effects caused by emulsifiers. According to the results, different extent of influences including the lipid content and lateral packing order state were observed after the treatments of PEGylated emulsifiers. The results obtained from the depth profiling analysis provided the possibility to estimate the least penetration depth of emulsifiers. Among them, PEG-20 ethers displayed the most penetration ability. Meanwhile, it is interesting to find that the treatment of emulsifiers can also affect the spatial distribution of  $D_2O$  whose differences were in line with the variations of skin lipid properties. Therefore, this study provides a systematic analysis for PEGylated emulsifiers and supports the possibility to use  $D_2O$  as a straightforward and cost-effective probe to evaluate the skin barrier function.

## Raman Imaging Analysis of Signaling Molecules in Mucoid and Non-Mucoid Strains of *Pseudomonas aeruginosa*

T. Cao, N. Morales-Soto, K. Kramer, J. Shrout, P. Bohn  
University of Notre Dame, Notre Dame, United States

*Pseudomonas aeruginosa* is an opportunistic human pathogen that can cause acute and chronic infections and diseases including cystic fibrosis (CF), especially among immune-compromised individuals. One characteristic of CF lung infection is the presence of a mucoid phenotype caused by alginate overproduction and this phenotype is closely related to quorum sensing (QS), a signal network that *P. aeruginosa* utilizes to coordinate cell group behaviors. Here, we focus on a clinical isolate mucoid strain of *P. aeruginosa*, named FRD1. We have specifically performed Raman imaging analysis to investigate spatiotemporal variations in the signal molecules (i.e. quinolones) of FRD1 quorum sensing system. By using this label-free technique, quinolone molecules were detected *in situ* and identified by the signature ring stretch vibrations within the 1330-1380 /cm spectral range using Raman micro-spectroscopy. We studied FRD1 under culturing conditions that both promote and limit the mucoid phenotype. Moreover, we compared FRD1 with 4 related strains (FRD1, FRD810, FRD440, FRD840 and FRD2), but with different mucoid/non-mucoid phenotypes and all strains were analyzed to inform the understanding of quinolone signaling during the mucoid to non-mucoid transition. Our results indicate that the *Pseudomonas* quinolone signal (PQS), one of the quinolone signal molecules, is universally activated at a longer stage across mucoid and non-mucoid strains, and most of the time after the appearance of 2-alkyl-4-hydroxyquinoline *N*-oxides (AQNOs) in mucoid cultures. This study highlights the distinct advantage of Raman imaging techniques in helping with passing the limitation of traditional biological techniques to acquire abundant spatiotemporal molecular information from bacterial communities. This approach will be useful to further examine PQS and other quorum sensing signaling during the transition of *P. aeruginosa* to the mucoid phenotype and other behaviors important to infection.

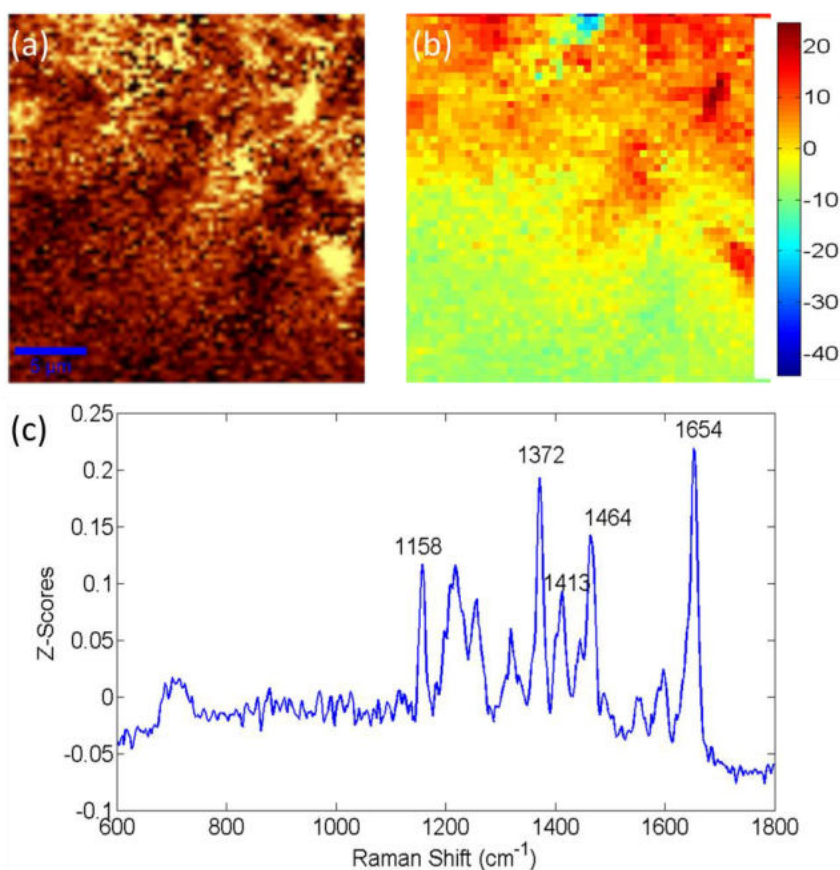


Figure 1. Raman imaging of FRD1 bacterial colony; (a) Raman image integrated over 1330-1380 /cm; (b) PCA mapping of the selected principal component (c) PCA loading plot of the selected principal component

## Confocal Raman imaging as a useful tool to understand the internal microstructure of multicomponent aerogels

I. Benito Gonzalez<sup>1</sup>, M. Martínez Sanz<sup>1</sup>, A. López Rubio<sup>1</sup>, L. G. Gómez Mascaraque<sup>2</sup>

<sup>1</sup>IATA (CSIC), Food Safety and Preservation Department, Valencia, Spain, <sup>2</sup>Teagasc Food Research Centre, Fermoy, Ireland

This work shows the characterization of (nano)cellulosic aerogels prepared from *Posidonia oceanica* waste biomass by means of confocal Raman microscopy (CRM). For this aim, aerogels were prepared using four (nano)cellulosic fractions with different purification degrees. These were then coated with polylactic acid (PLA) in order to improve their hydrophobicity and subjected to oil sorption–desorption experiments. Both univariate and multivariate analyses were compared in terms of the quality and the accuracy of the information provided. Univariate analysis only provided accurate information in the simplest systems (native (nano)cellulosic aerogels), while multivariate analyses facilitated the detection of the different components even for the most complex structures. Automatic identification of components was selected as the optimal methodology, although it also underestimated the abundance of the components with the least intense Raman spectra (cellulosic clusters) in the presence of more intense spectra such as PLA and oil. Micron-sized regions of concentrated cellulose were detected using CRM, being more abundant in the denser aerogels. Results also confirmed that PLA was preferentially located close to the surface, while oil could penetrate deeper along the matrix. Overall, the results showed the potential of Raman imaging as a novel approach for the characterization of complex biopolymeric aerogels.

### 3D quantitative Raman imaging of organoids

M. Barbero Mota<sup>1</sup>, V. LaLone<sup>2</sup>, A. A. Bharath<sup>1</sup>, K. Ritzau-Reid<sup>1</sup>, M. M. Stevens<sup>3</sup>

<sup>1</sup>Imperial College London, Bioengineering, London, United Kingdom, <sup>2</sup>Imperial College London, Bioengineering & Material Sciences, London, United Kingdom, <sup>3</sup>Imperial College London, Bioengineering & Material Sciences & Institute of Biomedical Engineering, London, United Kingdom

There is an increasing demand in biological sciences for a quantitative imaging tool that can unveil the biochemical 3D structure of bioconstructs. Tissue engineering clinical transfer requires thorough biochemical analysis in order to assess the exact physiomorphology of any biotechnology product. Raman microspectroscopy has been postulated as the ideal technique to meet this need. The emergence of more powerful hardware has enabled label-free non-invasive high-resolution imaging at the subcellular level. Until now, most Raman efforts have been qualitative, and those that offer quantification are limited to 2D analysis. One of the main reasons behind this remains the non-trivial computational task of quantitative spectra deconvolution in 3D, for which several algorithms have been proposed. Finding each biomolecular endmember contribution to the overall Raman spectrum is highly impaired by noise and depth interferences ligated to 3D specimens. In this study, we developed a novel quantitative calibration method which makes use of the Hybrid Least Squares (HLA) algorithm to provide reliable biochemical concentration quantification at each x-y-z position of 4% paraformaldehyde fixated 40-day human embryonic stem cell-derived brain organoids (hESC BO).

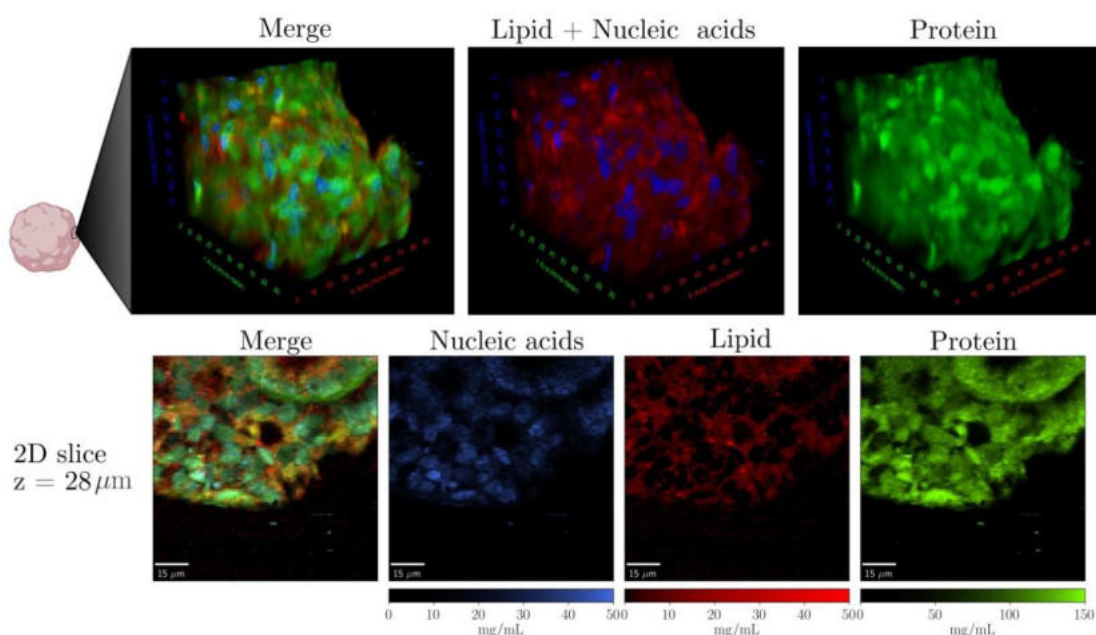


Figure 1 Brain organoid 80  $\mu\text{m}$  deep z-stack scan rendered into a 100\*100\*80  $\mu\text{m}$  representation. Merge, nucleic acids and lipid, and protein 3D quantitative channels are shown along with the 2D stack slice at 28  $\mu\text{m}$  z-value with biochemical concentration

HLA was selected out of seven machine learning algorithms by 10-fold cross-validation (10f-CV), including the chemometrics gold standards partial least squares and multivariate curve resolution alternative least squares. Artificially calibration datasets were derived from real Raman spectra contaminated with depth-noise levels simulating up to 80  $\mu\text{m}$  inside brain tissue. 10f-CV was run using the noisy datasets, and so error metrics vs depth profile was obtained for each model. HLA ranked top 2 on noiseless data (NRMSE = 0.25,  $R^2 = 0.935$ ), and also showed smooth profiles with depth that indicates HLA outstanding handling of stochastic shot noise. hESC BO 3D quantitative imaging results are shown in figure 1, nonetheless, this technique enables quantitative assessment of metabolic and structural phenomena underlying any 3D biospecimens.

## Raman spectroscopy of biomembranes for tissue engineering

S. Leal Marin<sup>1</sup>, O. Pogozykh<sup>2</sup>, C. Figueiredo<sup>2</sup>, B. Glasmacher<sup>1</sup>, O. Gryshkov<sup>1</sup>

<sup>1</sup>Gottfried Wilhelm Leibniz University of Hanover, Institute for Multiphase Processes (IMP), Garbsen, Germany,

<sup>2</sup>Hannover Medical School, Institute for Transfusion Medicine, Hannover, Germany

Extracellular matrix components (ECM), such as growth factors, collagen, glycoproteins and proteoglycans, are a key element in tissue engineering (TE) to support cell growth and proliferation. The inclusion of such components obtained from native tissues, such as the human amniotic membrane (hAM), into polymeric scaffolds has an advantageous application for the production of TE biomembranes. However, different chemical and physical hAM preservation methods as well as fabrication methods for the biomembranes, such as electrospinning, could affect the ECM structure and functionality. In this work, freeze-drying was evaluated as a promising approach for the preservation of ECM components in hAM, such as collagen and proteoglycans. The biomembranes were produced using electrospinning from 5% (w/v) poly(ethylene oxide) polymer and 2% (w/v) hAM dissolved in hexafluoroisopropanol. The analysis of the chemical composition of the unprocessed and freeze-dried hAM as well as produced biomembranes was performed using Raman spectroscopy (alpha300RA, Witec GmbH) using 532 nm laser, laser power 10 mW, 5s acquisition time, and 20 accumulations per point. The results presented the preservation of the main components of the hAM after freeze-drying such as collagen and some amides corresponding to proteoglycans. Besides, the mix of these components with the polymer was also traceable in the biomembranes. No shift in Raman peaks for the respective components was observed indicating the absence of chemical interaction between ECM components and the polymer. In conclusion, Raman spectroscopy allowed a simple and precise analysis of the preservation of the ECM components obtained from hAM after their inclusion in biomembranes obtained by electrospinning.

## Multi-bacteria, Multi-antibiotic, Testing Using Surface Enhanced Raman Spectroscopy (SERS) for Urinary Tract Infection (UTI) Diagnosis

K. Hadjigeorgiou<sup>1</sup>, E. Kastanos<sup>2</sup>, C. Andreou<sup>1</sup>, C. Pitris<sup>1</sup>

<sup>1</sup>University of Cyprus, Electrical and Computer Engineering, Nicosia, Cyprus, <sup>2</sup>Montgomery College, Biology Department, Rockville, United States

A urinary tract infection (UTI), a bacterial infection of the urinary tract, is one of the most common types of infections affecting more than 50% of women globally. Also, vulnerable to UTIs are chronically ill patients and children younger than two years old. Current diagnostic methods require 24 hours for the identification of the causative bacteria as well as an additional 24 hours for the determination of the most effective antibiotic. Because of these delays, doctors tend to prescribe broad-spectrum antibiotics until the official results of the diagnosis become available. The use of broad-spectrum antibiotics inevitably leads to ineffective treatments, recurrent infections, a significant financial burden to national healthcare systems and are responsible for antibiotic resistance. The aim of this research is to develop a fast and accurate method, based on Surface Enhanced Raman Spectroscopy (SERS), that could (i) detect if a sample is “positive” or “negative” for a UTI, (ii) classify the causative bacteria, found in the “positive sample”, according to their species, and (iii) determine the bacterial susceptibility to various antibiotics, all in a short time period. It should also allow correct classification of bacteria species coming directly from urine samples. The results of this research project provide a clear indication that, utilizing SERS, it is feasible to (i) detect the concentration of bacteria per sample, down to levels of  $10^3$  bacteria/ml, and determine the presence of a UTI, (ii) classify correctly the bacterial species with an accuracy of 93.75%, and (iii) identify antibiotic susceptibility within two to four hours of exposure with a correct classification ranging from 81.25 to 100%. These preliminary results can serve as the starting point for developing an innovative tool that could provide same day diagnosis and antibiogram for UTI, leading to more effective treatment with a significant socioeconomic impact.

## Silver nanoflower-coated paper for the determination of ketoprofen via surface enhanced Raman spectroscopy and ambient pressure paper spray mass spectrometry

M. C. Díaz-Liñán, M. T. García-Valverde, Á. I. López-Lorente, S. Cárdenas, R. Lucena

Departamento de Química Analítica, Instituto Universitario de Investigación en Química Fina y Nanoquímica IUNAN, Universidad de Córdoba, Campus de Rabanales, Edificio Marie Curie Anexo, E-14071, Córdoba, Spain

The use of paper has gained great attention in the last years due to its numerous advantages as support, such as low price, versatility and availability<sup>1</sup>. Furthermore, the easy handling of this type of material facilitates its coupling to different instrumental techniques, such as mass spectrometry or surface enhanced Raman spectroscopy (SERS), among others. Regarding SERS, the use of plasmonic nanoparticles with sharp edges<sup>2</sup>, e.g. gold and silver, has increased since a high number of the so called hot spots are formed, which lead to strong electromagnetic confinement, thus significantly increasing the low interaction cross sections observed in vibrational spectroscopies such as Raman spectroscopy. Furthermore, the presence of a metal is also important in more recent approaches like paper spray, since it is based on a difference of potential. This technique allows direct analysis of samples, thereby simplifying the analytical process, since sample pretreatment is avoided<sup>3</sup>.

In this context, a dual substrate for both SERS and ambient pressure paper spray mass spectrometry (PS-MS) based on the modification of filter paper with silver nanoflowers (AgNFs) has been developed. In the early stage of the synthesis, filter paper was coated with nylon-6 and incubated in ethylenediamine, which acts as an anchor point for the nanoflowers. The as synthesized substrate was characterized via scanning electron microscopy and infrared spectroscopy. The densely packed petals of the AgNFs led to a great amount of hot spots, resulting in an enhancement not only in the Raman signal, but also in the sensitivity of the mass spectrometric analysis compared to bare paper and nylon/Ag-coated paper.

<sup>1</sup> Jiang, X.; Fan Z.H. *Annual Rev. Anal. Chem.*, **2016**, *9*, 203.

<sup>2</sup> Bibikova, O.; Haas, J.; López-Lorente, A.I.; Popov, A.; Kinnunen, M.; Meglinski, I.; Mizaikoff, B. *Analyst*, **2017**, *142*, 951.

<sup>3</sup> Wang, H.; Liu, J; Graham Cooks, R.; Ouyang, Z. *Angewandte*, **2010**, *122*, 889.

***Gold Nanoparticles contaminated by Bacterial Endotoxin: biophysical characterization, imaging and nanotoxicology***

A. Verde, M. Mangini, P. Italiani, D. Boraschi, A. C. De Luca  
National Research Council of Italy, Institute of Biochemistry and Cell Biology, Naples, Italy

Gold nanoparticles (AuNPs) are nanodevices that can have many uses in biomedical applications but unfortunately they show in some cases nanotoxic effects on biological systems [1]. Among the different AuNPs effects in cells, activation of immune responses is considered a central issue for assessing health risks of AuNPs [2]. The main goal of this study is to identify and analyse the activation of the inflammatory response associated to gold nanoparticles and/or to the presence of bacterial endotoxin (or Lipopolysaccharide, LPS) on the nanoparticles' surface. To this aim, the interaction of AuNPs with LPS is analysed, the presence of LPS molecules on NPs is quantified, and the interaction of AuNPs with human primary macrophages is investigated, in order to distinguish the intrinsic NPs biological effects from those induced by LPS.

LPS dose-dependent adsorption on 50 nm AuNPs was studied by DLS and SERS in order to understand the amount of LPS that binds to NPs surface and quantify it. Internalization of bare and LPS coated 50 nm AuNPs was studied in macrophages by Raman imaging [3] and their inflammatory effect was studied by in vitro stimulation through evaluation of inflammatory cytokine production (TNF- $\alpha$ ).

DLS results indicate that a uniform LPS corona (8712 molecules) is formed around all NPs (2  $\mu$ g) when incubated with doses greater than 500 ng, while analysis of SERS signals show a Limit of Detection (LOD) for LPS amount of the order of fg. These promising results show how SERS technique can be a reliable LPS-Sensor, while NPs imaging studies showed that NPs are localized in cytoplasmic vesicles inside macrophages. Moreover, bare NPs do not induce the production of TNF- $\alpha$  cytokine in treated macrophages.

[1] Chen, YS., Hung, YC., Liao, I. et al. "Assessment of the In Vivo Toxicity of Gold Nanoparticles" *Nanoscale Res Lett* (2009) 4: 858

[2] Boraschi, D. and A. Duschi. 2012. "Immune System. In *Adverse Effects of Engineered Nanomaterials*" edited by B. Fadeel, A. NANOTOXICOLOGY 1173 Pietroiusti, and A.A. Shvedova, 169–184. Amsterdam:Academic Press.

[3] Managò, S. Migliaccio, N. Terracciano, M. Napolitano, M. Martucci, M. N. De Stefano, L. Rendina, I. De Luca, A. C. Lamberti, A. Rea, I. "Internalization kinetics and cytoplasmic localization of functionalized diatomite nanoparticles in cancer cells by Raman imaging" *J. Biophotonics*. 2018; 11: e201700207

## Elucidating the composition of micro-scale polymer scaffolds for biomedical applications by confocal Raman microscopy

T. Kielholz, F. Rohde, M. Walther, M. Windbergs

Institute of Pharmaceutical Technology and Buchmann Institute for Molecular Life Sciences, Goethe University, Frankfurt am Main, Germany

### Introduction:

Fiber-based scaffolds are gaining increasing importance as drug delivery systems as well as for tissue engineering due to their easily tunable chemical composition, fibrous structure and favorable mechanical properties. However, especially in case of multi-component-systems, analytical characterization is challenging with respect to differentiation of individual components. As integration of labels in such systems is prone to modify the physicochemical behavior of the polymers and labeling after fabrication in three-dimensional scaffolds is challenging, we aimed to evaluate confocal Raman microscopy in terms of its applicability for multicomponent micro-scale polymer scaffolds.

### Materials & Methods:

Samples with two distinct fiber types were fabricated via parallel electrospinning of organic polymer solutions containing polycaprolactone (PCL) and poly(lactic-co-glycolic acid) (PLGA). An Alpha 300R+ confocal Raman microscope (WITec GmbH, Ulm, Germany) equipped with a 532 nm laser was used to analyze the pristine fiber mats. Raman scans in x- and y-direction as well as for acquisition of multiple z-layer scans were acquired to assess the three-dimensional organization of the sample. Adjacent evaluations were performed with hierarchical clustering and basis analysis.

### Results:

PCL/PLGA fiber mats were fabricated and Raman imaging was successfully used to differentiate the individual fiber based on their composition. While PCL fibers showed a uniform appearance, individual PLGA beads could be detected. Based on this information, the process parameters were optimized. Raman analysis of the optimized fiber mat visualized uniform fibers without any bead formation. Interestingly, the corresponding false-color image also showed significantly larger fiber diameters for PCL than PLGA. A three-dimensional model was generated based on Raman data of z-stacks and proved the spatial homogeneous polymer distribution up to the entire cross-section of the sample.

### Conclusion:

Confocal Raman microscopy successfully visualized polymer distribution and existing manufacturing defects. Visualizing the composition was crucial for gaining an in-depth understanding of the scaffold itself and determining subsequent steps for process improvement. The method offers great potential to analyze not only fibers but also a plentitude of multi-component polymer specimens.

## SERS imaging via metasurface made of silver-silicone periodic disks

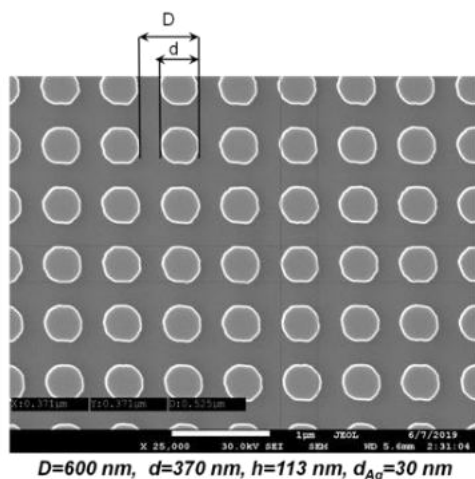
A. Ivanov, I. Bykov, I. Ryzhikov, I. Boginskaya, A. K. Sarychev

Institute for Theoretical and Applied Electrodynamics, Russian Academy of Sciences, Moscow, Russian Federation

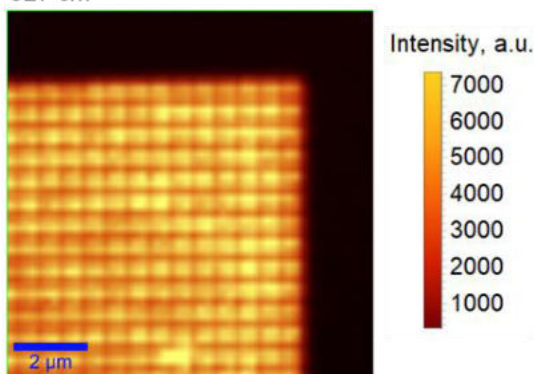
We investigate the light interaction with the regular metasurface made of silver-silicone periodic disk resonators. Computer simulations as well as real experiment reveal an anomalous optical response of the metasurface, which is due to the excitation of various metal-dielectric surface plasmons. The enhancement of the local electric fields was measured from distribution of the Raman scattering signals over the surface. We demonstrate SERS imaging of the metasurface made of silver-silicone periodic disks. Raman signals excited by 785 nm laser radiation were recorded with a WiTec spectrometer (WiTec 500 Alpha) using mapping regime. The Raman spectrum is collected with 100x objective (NA=0.9), mapping area  $50 \times 50 \mu\text{m}^2$ , step of scanning  $0.56 \mu\text{m}$ , depth of focus  $0.5 \mu\text{m}$ . We focused on crystalline silicon band  $527 \text{ cm}^{-1}$  to demonstrate the enhancement of local electric fields over the metasurface.

The optical mapping of the intensity distribution for the Raman line  $527 \text{ cm}^{-1}$  of silicon is shown on Figure. The result of the optical mapping was compared to the coordinate grid scanning electron microscopy (SEM) to find the signal from each point of the surface. We demonstrate a significant enhancement of the intensity distribution in the metasurface with respect to flat region. Moreover, the distribution of hot spots generated by silver-silicon disks repeats the morphology of the surface, which is shown on SEM image. The metasurface allows to reach the SERS enhancement factor of several orders of magnitude and very stable signal with uniform local electric field distribution over the entire surface. Therefore the system is much more thermally stable than most known SERS substrate, where molecules of an analyte degradate in the hot spots.

SEM image of silver-silicone periodic disks



Optical mapping of the intensity distribution of silicon Raman spectral line with Stokes shift  $527 \text{ cm}^{-1}$



The work was partially supported by Russian Academy of Sciences (grant No. 20-21-00080) and Russian Science Foundation (grant No. 16-14-00209).

## Chemically-selective visualisation of organoids and their interaction with hydrogel matrices

N. Jung<sup>1</sup>, T. Moreth<sup>2</sup>, F. Pampaloni<sup>2</sup>, E. H. K. Stelzer<sup>2</sup>, M. Windbergs<sup>1</sup>

<sup>1</sup>Goethe University, Institute of Pharmaceutical Technology and Buchmann Institute for Molecular Life Sciences, Frankfurt am Main, Germany, <sup>2</sup>Goethe University, Buchmann Institute for Molecular Life Sciences, Frankfurt am Main, Germany

*In vitro* cell culture systems in 2D and 3D environments have experienced a surge in popularity over the last decades in the growing field of alternative approaches to animal testing. Especially the cultivation of organoids represents a promising approach in various clinical applications and with respect to personalised medicine. Although the development of physiological relevant cellular systems is evolving steadily, approaches for their comprehensive characterisation are stagnating, relying on bright-field based visualisation and fluorescence-based imaging approaches. While the one delivers only limited information, the other requires fixation and staining procedures, which are often impeded by the surrounding extracellular matrix (hydrogels). In order to gain a comprehensive understanding of organoid cultures, their development and especially their interaction with the surrounding matrix, which is neglected in the established analyses, confocal Raman microscopy was implemented in the here presented study. Mouse pancreas organoids, embedded in three different hydrogel matrices (commercial Matrigel® and two synthetic hydrogels), were analysed on single cell level as well as on whole organoid level to determine matrix-dependent developmental alterations. We were able to show the sub-cellular organisation of single pancreas cells and the distribution of organelles and nucleic acids and further evaluate the interaction of single organoids with the surrounding matrix by imaging the interface between organoid and hydrogels. Based on these results, suitable synthetic hydrogels could be identified as alternatives to the animal-derived, established Matrigel® and a spectroscopy-based analysis procedure was established to allow for high-throughput analyses of whole organoid cultures. Due to the label-free and chemically-selective nature of the technique, we show for the first time that it is possible to analyse 3D cell culture systems in their native state within a hydrogel matrix and provide a glimpse into the possibilities of confocal Raman microscopy as an innovative approach for the analysis of hydrogel-based 3D *in vitro* cell culture systems.

## A Raman-based approach for detecting circulating tumor cells.

M. Mangini<sup>1</sup>, M. A. Ferrara<sup>2</sup>, G. Zito<sup>2</sup>, S. Managò<sup>1</sup>, A. Luini<sup>1</sup>, G. Coppola<sup>2</sup>, A. C. De Luca<sup>1</sup>

<sup>1</sup>Institute of Biochemistry and Cellular Biology, Naples, Italy, <sup>2</sup>Institute of Applied Sciences and Intelligent Systems, Naples, Italy

Circulating tumor cells (CTCs) are a rare subgroup of cells that detach from the primary solid tumor and circulate in the bloodstream of cancer patients. These cells act as a seed for metastases; moreover, they maintain the primary tumor heterogeneity and mimic tumor properties. All these features make CTCs good candidates to be used as clinical biomarker for patient diagnosis, prognosis and treatment. Indeed, the isolation and characterization of CTCs can smooth the way to apply precision medicine approach in cancer patients. However, the current methods to detect CTCs are mainly based on the recognition of epithelial cell adhesion molecule (EpCAM) expressed on cancer cell membrane, but they typically fail to detect tumoral cells that are losing epithelial phenotype and starting invasion/metastatic process. Here, we used deuterium as vibrational tag to develop a new CTCs detection method based on Raman spectroscopy potentially able to detect any type of CTCs. In particular, we exploited the capacity of cancer cell to internalize and metabolize glucose 5-10 faster than normal cell, the so-called Warburg effect. Normal prostatic cells (PNT2), cancer prostatic (PC3) and hepatic (HepG2) cells were used as *in vitro* model. Cells were cultured in presence of 25mM deuterated glucose for 48h and then analyzed by Raman spectroscopy (1). The typical deuterium Raman band at 2100  $\text{cm}^{-1}$  was present in the spectra of PC3 and HepG2 cells, but not in PNT2 spectra. These results indicate the presence of Warburg effect in our cellular model and that cancer cells can be differentiated from normal cells following glucose metabolism. To simulate the presence of CTCs in blood, PC3 and HepG2 cells were co-cultured with white blood cells isolated from healthy donor blood in presence of deuterated glucose. The deuterium Raman signal was observable only in the spectra of PC3 and HepG2 cells. Our data demonstrate that cancer cells can be distinguished from healthy cells independently from EpCAM expression just exploiting the glycolytic metabolism also when they are in the same media. These results shed a light on the possibility to develop new CTCs detecting methods using label-free approach based on Raman spectroscopy.

1. Managò S., Valente C., Mirabelli P., Circolo D., Basile F., Corda D. and De Luca A.C, 2016. A reliable Raman-spectroscopy-based approach for diagnosis, classification and follow-up of B-cell acute lymphoblastic leukemia. *Sci Rep.* 19, 6:24821.

## Raman imaging of the functional adipose tissue

Z. Majka, K. Czamara, A. Kaczor  
Jagiellonian University, Kraków, Poland

For many years, the adipose tissue, particularly the perivascular adipose tissue (PVAT), was disregarded by anatomopathologists as incoherent and irrelevant.<sup>1</sup> Nowadays, it is certain that PVAT is markedly involved in vascular homeostasis.<sup>2</sup> Depending on its phenotype, PVAT has different functions, *inter alia*, anti-inflammatory action and regulation of insulin sensitivity.<sup>3</sup> PVAT can be reminiscent of interscapular brown adipose tissue (iBAT) in the thoracic aorta (TA PVAT) or epididymal white adipose tissue (eWAT) in the abdominal aorta (AA PVAT). Moreover, PVAT dysfunctions may lead to inflammation, dyslipidemia and insulin resistance.<sup>3</sup> All these diseases can contribute to the increased cardiovascular risk associated with obesity, which is a common cause of mortality in the world.<sup>2,3</sup> Therefore, it is important to find an effective method to determine pathological changes in the adipose tissue. Due to large Raman scattering cross-section of lipids, Raman spectroscopy is well fitted tool to investigate the adipose tissue.<sup>4</sup>

The aim of this work was to investigate the processes involved in obesity development i.e. inflammation and excessive lipid accumulation. We developed the *in situ* adipose tissue model for investigation of chemical changes in the functional adipose tissue stimulated by various factors. The chemical composition of the adipose tissue of healthy mice isolated from different depots (iBAT, eWAT, TA PVAT, AA PVAT) was visualized *in situ* using Raman imaging after 24 and 48 hours incubation in medium supplemented with saturated fatty acids or inflammatory factor i.e. TNF-alpha. The analysis of Raman images enabled to show individual adipocytes and the intercellular matrix and to study changes in lipid content and lipid unsaturation based on Raman marker bands. This work demonstrates the potential of Raman imaging in studies of single adipocytes *in situ* in the functional adipose tissue.

1. C. M. Pond, *Front. Physiol.*, 2017, **8**, 8–10.

2. K. Schäfer, I. Drosos and S. Konstantinides, *Int. J. Obes.*, 2017, **41**, 1311–1323.

3. M. S. Fernandez-Alfonso, B. Somoza, D. Tsvetkov, A. Kuczmani, M. Dashoowd and M. Gil- Ortega, *comprehensive Physiol.*, 2018, **8**, 23–59.

4. K. Czamara, Z. Majka, M. Sternak, M. Koziol, R. B. Kostogryś, S. Chlopicki and A. Kaczor, *Int. J. Mol. Sci.*, 2020, **21**, 1–14.

## Glioma Tumors Classified using Visible Resonance Raman Spectroscopy and Machine Learning

Y. Zhou<sup>1</sup>, S. Zhang<sup>2</sup>, L. Zhang<sup>1</sup>, B. Wu<sup>3</sup>, K. Zhu<sup>4</sup>, C. Zhang<sup>5</sup>, Y. Yang<sup>4</sup>, X. Yu<sup>6</sup>, H. Hu<sup>7</sup>, C.-h. Liu<sup>5</sup>, R. Alfano<sup>5</sup>  
<sup>1</sup>Air Force Medical Center, Beijing, China, <sup>2</sup>JRME Co., Ltd., Taizhou, Jiangsu, China, <sup>3</sup>Southern Connecticut State University, Physics, New Haven, United States, <sup>4</sup>Chinese Academy of Sciences (CAS), Beijing, China, <sup>5</sup>City College of New York, New York, United States, <sup>6</sup>General Hospital, Beijing, China, <sup>7</sup>WITec GmbH Beijing Rep. Office, Beijing, China

Human glioma is an advanced disease which accounts for 75% of all newly diagnosed malignant primary brain tumors, with an average survival time of about one year. Early diagnosis and detection of glioma is still desired for initial treatment.

In this study, we report a new optical molecular histopathology method based on visible resonance Raman (VRR) spectroscopy combined with confocal Raman microscopy (CRM) for diagnosing human brain glioma and distinguishing gliomas of grades II through IV from normal brain tissues.

VRR is a novel label-free technique for optical molecular histopathology assay started in 2011. VRR Raman signals are enhanced due to “magic” 532nm excitation wavelength which matches a large group of natural biological molecular absorption bands. CRM offers a new way to identify cancers from normal tissues with high resolution, non-destructive molecular mapping and provided hyperspectral images with highly complex biochemical and physiological information of biological tissues. This is different from traditional optical imaging.

VRR images from twenty-five specimens including healthy tissues and gliomas of grades II to IV were investigated *ex vivo* using WITec300R confocal micro Raman imaging system with laser excitation of 532nm. Two-dimensional (2D) RR spectral mappings performed in 20 $\mu\text{m}$ ×20 $\mu\text{m}$  with a step size of 1 $\mu\text{m}$  generated a dataset of 400 spectra which is essentially an image stack with Raman shift as the third dimension and shows the distribution of various biochemical bonds in image slices. A three-dimensional (3D) plot was used to demonstrate the spatial distributions of three selected sets of molecular biomarkers and revealed significant differences in the components between normal and different grades of gliomas due to the chemical composition changes. The RR molecular spectral fingerprints showed (a) a clear enhancement of vibrational modes at 1129 and 1338 $\text{cm}^{-1}$  which are believed to arise from lactate and DNA; (b) an evident decrease in the RR vibrational modes at 1442 and 2854/2885 $\text{cm}^{-1}$  due to saturated fatty acids bonds (proteolipid) in all-grades of glioma tissues compared with normal tissues; and (c) an enhancement in the RR spectral modes of 1129 and 2938 $\text{cm}^{-1}$  (saccharolipids) which suggests the contribution from lactate. These findings may provide a novel proof for anaerobic glycolysis metabolic process in brain gliomas which has been explained by Warburg effects. An example of VRR imaging result is shown in Fig. 1.

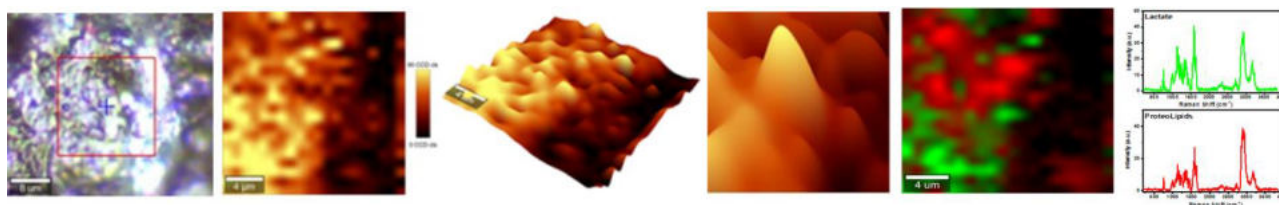


Fig. 1. VRR imaging of grade II glioma. From left: brightfield image; VRR 2D image for 1129 $\text{cm}^{-1}$ ; VRR image using 3D plot; 3D image zoomed-in; color-coded image based on spectra of the components and the corresponding spectra of lactate and lipids

## Biopharmaceutical structural characterization by Confocal Raman methodology: Defining critical parameters to method development

J. Silva, J. Cristóvão, J. Pereira

Hovione Farmaciência S.A., Estrada do Paço do Lumiar, Campus do Lumiar, Edifício S, 1649-038 Lisboa, Portugal, R&D - Analytical Development, Lisbon, Portugal

Confocal Raman microscopy and spectroscopy are powerful techniques for solid-state protein pharmaceutical analysis that can be used for identity and stability testing, being useful to determine changes in the secondary and tertiary structure of proteins in different matrices<sup>1</sup>. Raman spectrometry has significant potential advantages in Biopharmaceutical industry, as intrinsically high molecular specificity, flexibility of sampling configurations and the requirement for minimal (or no) sample pre-treatment and can be exploited to deliver unique and useful analytical solutions. However, Raman-based methods, when applicable to proteins, can be limited by the chemical complexity of those. Nevertheless, with enough knowledge on the proteins structure and good experimental design, robust analytical methods can be developed. The present work aims to define a systematic approach for method development of Confocal Raman spectroscopy by means of Analytical Quality by Design (AQbD) that could be used to a wide range of protein-based molecules aiming at detecting discrete changes in conformational structure. In this presentation, the work conducted regarding the development of an ID method for proteins, following an AQbD approach, is shown. To develop an analytical method for the identification of proteins secondary structure, Bovine Serum Albumin (BSA), was defined as model protein. The goal is to later on apply this method for Amide I, Amide III and Skeletal Stretch – hence the typical wavelengths regions of these proteins<sup>2,3</sup> were selected for fingerprint. Spectra accumulations and integration time were identified as Critical Method Parameters (CMP) (Figure 1a); normalized areas of the zones of interest, as well as corresponding standard deviations were found to be critical method attributes. With the defined success criterion, we were able to achieve a Method Operable Design Region (MODR) (blank region on Figure 1b). To confirm the robustness of the method and the consistency of the analytical target profile, a second DoE (Figure 1c) was performed - results obtained were in line with expectations (Figure 1d).

AQbD methodology was successfully used as an effective and comprehensive tool for Raman spectroscopy ID method development of complex systems. In fact, with this approach, it was possible to optimize the critical method attributes and define the most robust conditions of analysis.

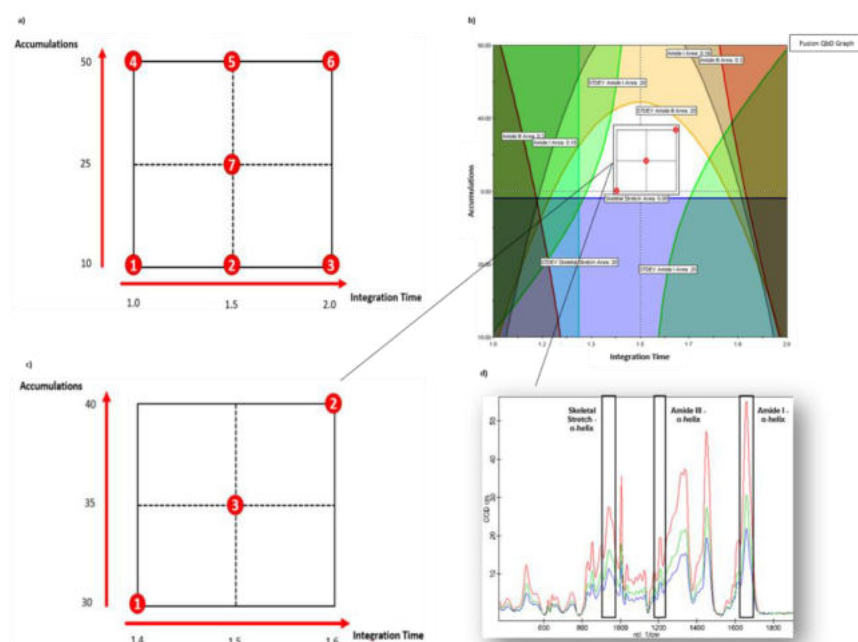


Figure 1 - a) DoE to define CMP; b) Experiment prediction in Fusion QbD® software; c) DoE to prove robustness; d) Resulting spectra with zones of interest (red: 30 acc./1.4s int. time; green: 40 acc./1.6s int. time; blue: 35 acc./1.5s int. time)

## Visualization of extractives and xylan-type polysaccharides in ivory nut endosperm by Raman imaging and principal component analysis

Y. Ferreira da Silva<sup>1</sup>, R. Nunes Oliveira<sup>2</sup>, R. Antoun Simão<sup>1</sup>

<sup>1</sup>Federal University of Rio de Janeiro, Department of Metallurgical and Materials Engineering, Rio de Janeiro, Brazil,

<sup>2</sup>Federal Rural University of Rio de Janeiro, Department of Materials Engineering, Seropédica, Brazil

In advance of World War II and the widespread consumption of synthetic polymers, ivory nuts were a prevalent source of income to South American countries such as Ecuador, Colombia and Brazil. These seeds, produced by palms from the genus *Phytelephas*, present a rigid endosperm that was exported as a raw material for the fabrication of buttons. However, the economic impacts of the war reduced their international trade, which was not reestablished due to popularization of plastics. Nowadays, the awareness of environmental issues caused by synthetic polymers has restored the interest in natural materials, and ivory nuts have been lately investigated due to their noteworthy mechanical properties and eco-friendly appeal. Their endosperm, previously characterized by wet chemical methods, has been reported as constituted by pure mannan, biopolymer based on mannose with a low degree of substituents, and a minor amount of cellulose. However, the characterization by chemical extractions may modify the original cell wall structure and add artifacts to the results. Hence, in this work, ivory nut endosperm was characterized by Raman imaging to identify cell wall constituents non-destructively and visualize their spatial distribution. Ivory nut disks with polished surfaces were analyzed in a Witec Alpha 300 Raman spectrometer using a 785 nm laser and a 10 x objective lens with a 0.30 numerical aperture. Hyperspectral imaging maps were generated in a 50 x 50  $\mu\text{m}^2$  region and spectral processing was performed using Witec Project 2.10 and RStudio, as illustrated below.

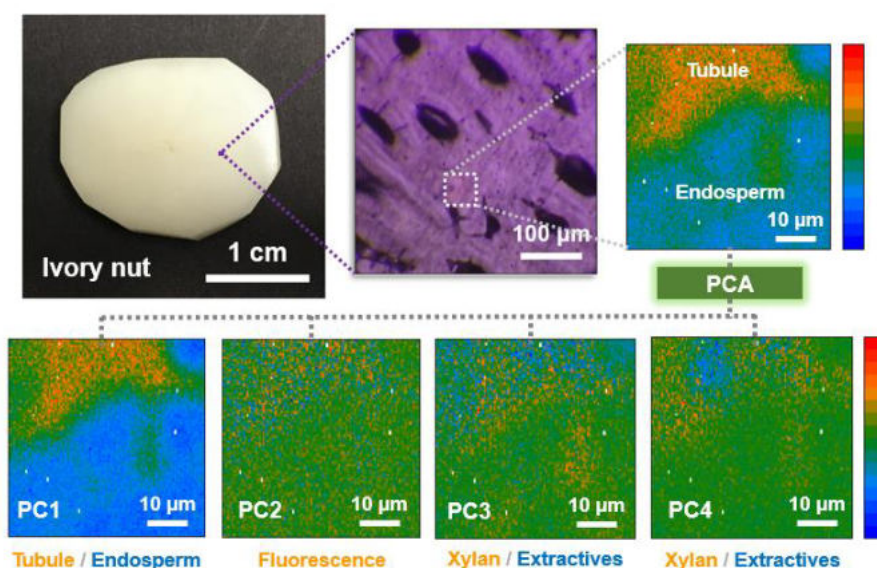


Diagram illustrating ivory nut sample, an optical microscopy image and an average intensity map for Raman imaging in the analyzed region. In addition, PCA average intensity score maps are provided.

The average spectrum in the 1000 to 1750  $\text{cm}^{-1}$  range mainly contained peaks attributable to xylan-type polysaccharides (1021, 1081, 1106, 1134, 1246, 1311 and 1364  $\text{cm}^{-1}$ ), cellulose (1454  $\text{cm}^{-1}$ ) and lipids (1466  $\text{cm}^{-1}$ ). Besides, overlapped contributions from  $\beta$ -mannose units (1081, 1106 and 1134  $\text{cm}^{-1}$ ) and  $\beta$ -glucose units (1106  $\text{cm}^{-1}$ ) could also be present. In order to evidence subtle spectral contributions and distinguish overlapped peaks, principal component analysis (PCA) was performed using RStudio and hyperspec package. PCA results for the first four principal components evidenced the accumulation of xylan and extractives, specially waxes and polar compounds, in endosperm tubules. These results indicate that, besides mannan and cellulose, ivory nut cell walls are constituted by xylan-type polysaccharides while endosperm tubules contain extractive substances, probably present as a defense to biodeterioration.

## Customizable SERS substrates dedicated for life science and diagnostic research

P. Albrycht<sup>1</sup>, J. Borkowska<sup>2,3</sup>, M. Książopolska-Gocalska<sup>3</sup>, Ł. Kozoń<sup>3</sup>, R. Hołyst<sup>3</sup>

<sup>1</sup>Institute of Physical Chemistry PAS, Soft Condensed Matter, Warsaw, Poland, <sup>2</sup>Mossakowski Medical Research Centre Polish Academy of Sciences, Warszawa, Poland, <sup>3</sup>Institute of Physical Chemistry PAS, Warsaw, Poland

Surface-Enhanced Raman Spectroscopy (SERS) is gaining popularity in life sciences as it allows us to obtain the fingerprint of a specific substance or even of a cell type. Thus, SERS is now intensively studied as a promising tool for diagnostic and pathogen identification. SERS-based biosensors and microfluidic systems may be fast (a few seconds measurements) and accurate platforms for detecting cancer, food contamination, and even viruses identification.

We have recently developed sensitive and repeatable silver and silver-gold SERS substrates dedicated to potential use in biosensors and microfluidic systems for diagnostic, forensics, and life science research. Substrates are made by the electrodeposition of silver and gold nanoparticles on ITO glass. Our substrates have dimensions dedicated to 96-well plates and give excellent (ppm to ppb) enhancement after compound deposition in a small volume of analyzed solution. Additionally, thanks to the use of a precise laser plotter, we can obtain defined dimensions of substrates. It is especially desirable for the development of "Lab-on-a-Chip" type platforms. Our SERS substrates can have hydrophilic or hydrophobic properties (on demand). Substrates with a hydrophilic surface give excellent enhancement of aqueous solutions, while hydrophobic substrates are dedicated to alcoholic solutions.

# Confocal Raman Microscopy

## 2<sup>nd</sup> Edition

Confocal Raman Microscopy, edited by members of the WITec team and part of the Springer Series in Surface Sciences, has been thoroughly revised and expanded for its 2<sup>nd</sup> edition. The book provides a comprehensive overview of the fundamentals, practical considerations and real-world applications of Raman microscopy.

With 23 chapters it also includes sub-sections on theory and technology, novel materials, geosciences, life and pharmaceutical sciences, materials science and a historical overview of the Raman effect.

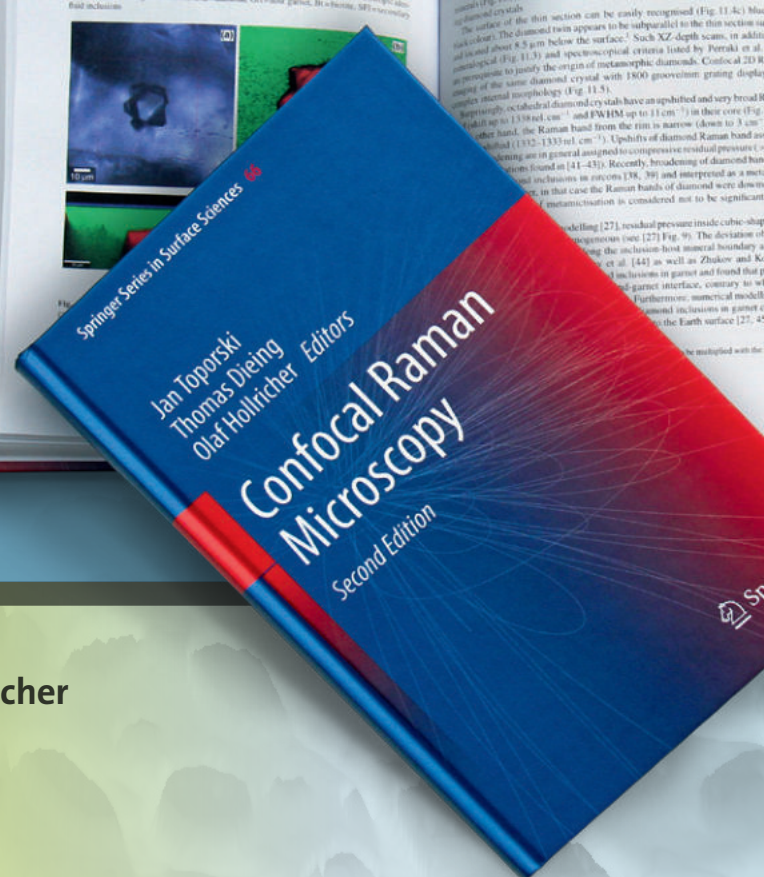
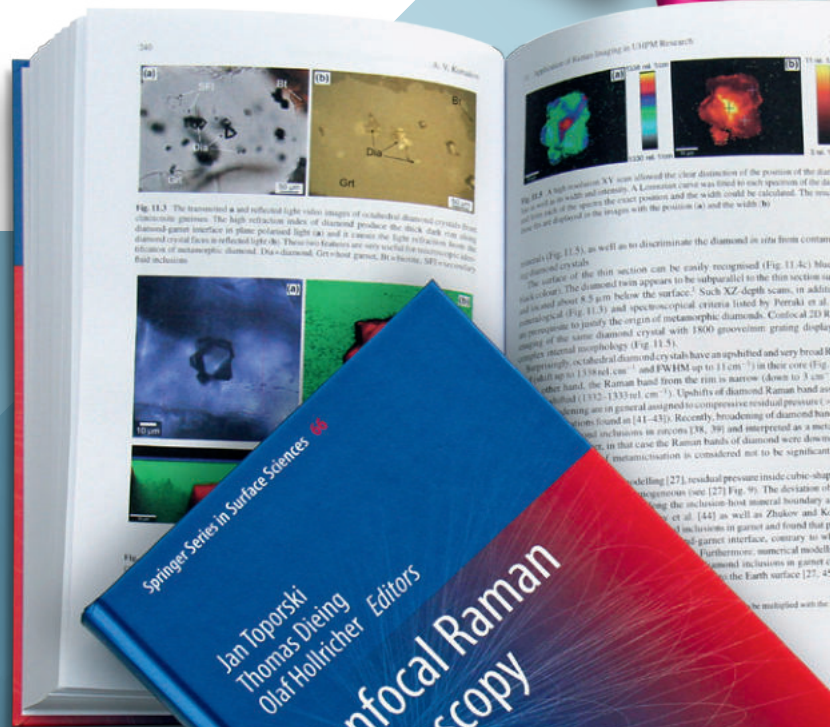
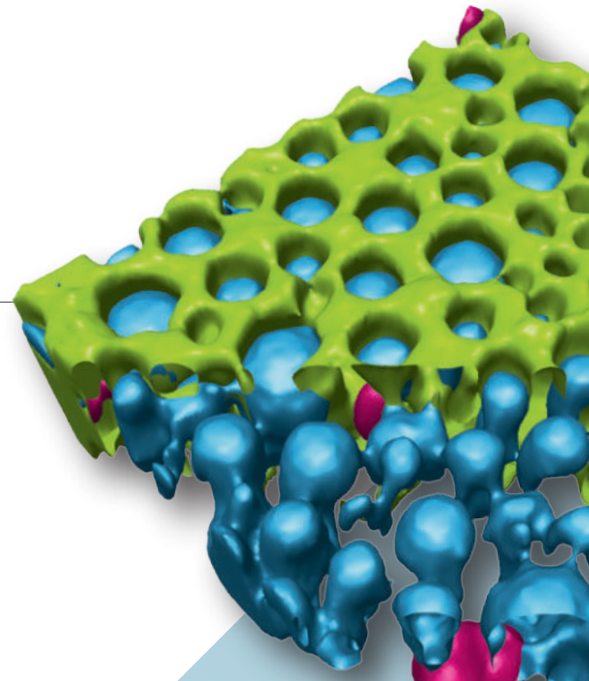
Additionally, it explores the rapidly evolving field of correlative microscopy by detailing how 3D Raman imaging can be integrated with other investigative methods to achieve a far greater understanding of a sample's properties.

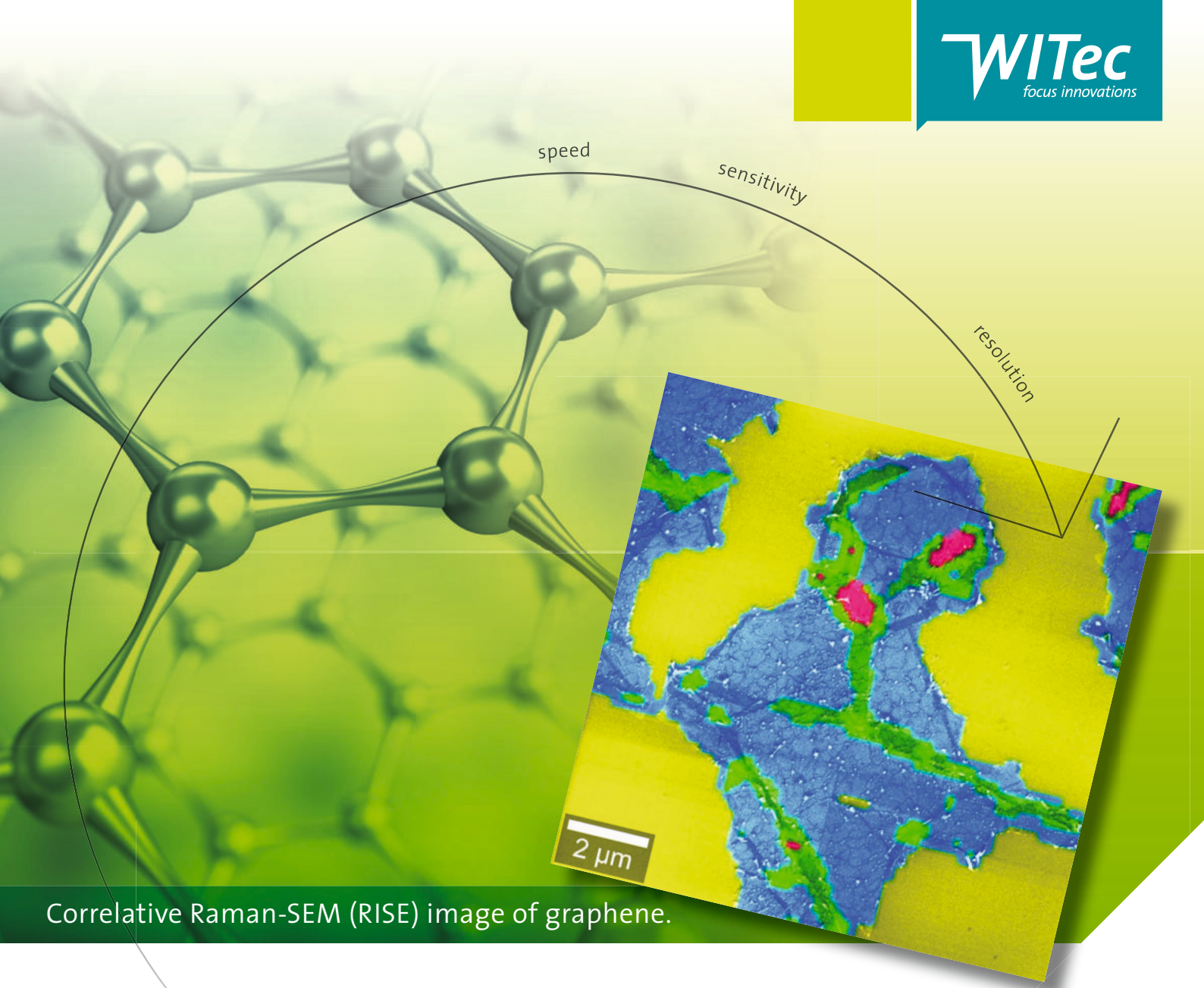
The 2<sup>nd</sup> edition of Confocal Raman Microscopy, edited by WITec scientists Dr. Olaf Hollricher, Dr. Thomas Dieing and Dr. Jan Toporski, can be purchased in print or e-book formats directly from Springer or through online shops.

**Order your copy today and have the current state of the art in Confocal Raman Microscopy at your fingertips.**

**Confocal Raman Microscopy**  
**Editors: Jan Toporski, Thomas Dieing, Olaf Hollricher**  
**ISBN: 978-3-319-75380-5**

[www.witec.de](http://www.witec.de)





Correlative Raman-SEM (RISE) image of graphene.

# 3D Raman Imaging

Turn ideas into **discoveries**

Let your discoveries lead the scientific future. Like no other system, WITec's confocal 3D Raman microscopes allow for cutting-edge chemical imaging and correlative microscopy with AFM, SNOM, SEM or Profilometry. Discuss your ideas with us at [info@witec.de](mailto:info@witec.de).



Raman · AFM · SNOM · RISE

[www.witec.de](http://www.witec.de)